Geomorphology 101 (2008) 14–32

Contents lists available at ScienceDirect

Geomorphology

journal homepage: www.elsevier.com/locate/geomorph

Late Quaternary hydroclimatology of a hyper-arid Andean watershed: Climate change, floods, and hydrologic responses to the El Niño-Southern Oscillation in the Atacama Desert

F.J. Magilligan [a,*], P.S. Goldstein [b], G.B. Fisher [c], B.C. Bostick [d], R.B. Manners [e]

[a] Department of Geography, Dartmouth College, Hanover, NH, 03755, United States
[b] Department of Anthropology, University of California, San Diego, La Jolla CA 92093-0532, United States
[c] Department of Earth Sciences, University of California, Santa Barbara, CA 93106, United States
[d] Department of Earth Sciences, Dartmouth College, Hanover, NH, 03755, United States
[e] Inter-Fluve, Inc., 1020 Wasco Street, Hood River, Oregon, 97031, United States

ARTICLE INFO

Article history:
Accepted 22 April 2008
Available online 25 May 2008

Keywords:
El Niño
Andes
Floods
Climate change
Isotopes
Tiwanaku

ABSTRACT

Although certain characteristics of the El Niño-Southern Oscillation (ENSO) are well known on contemporary timescales, less is known about the magnitude–frequency relationships of this atmospheric phenomenon on longer timescales or its relationship to widespread flooding, especially in its core zone along the sub-tropical Andes where La Niña or El Niño episodes control regional hydroclimatology. Using a combination of stratigraphic evidence, geochronologic dating (^{14}C and OSL), stable isotope analyses, and water geochemistry along the Rio Moquegua in the northern fringes of the Atacama Desert, we assemble a paleoflood chronology for mainstem and tributary sections for the past ca. 20 ka and ascertain the variation in ENSO frequency and magnitude. Because of the inherent watershed structure and regional hydroclimatology, mid-valley tributaries of the Rio Moquegua only flood during El Niño episodes and thus provide an important proxy of extreme El Niños while mainstem stratigraphy records both La Niña and El Niño episodes. El Niño floods appear to have been pronounced during the Late Pleistocene and up to at least the Younger Dryas (~12,000 cal yr BP) while stratigraphic evidence of large El Niño floods is lacking in tributary systems during the Mid-Holocene.

Flood stratigraphy in a ~2 ka 7 m high terrace along the mainstem indicates an increased frequency and magnitude of large floods between ca. 700 and 1610 AD as compared to the period from ca. 160 BCE to 700 AD with "mega-Niños" occurring ca. 1330 AD and ca. 1650 AD. Water geochemistry and radiocarbon dating indicate that at least two major aquifers exist, with wells and springs in the mid-valley dating to 710 and 3100 ^{14}C yr BP, respectively, while water from a spring in the headwaters dates to 10,320 ^{14}C yr BP. This range in dates suggests that groundwater flow in the mid-valley is neither fossil water nor exclusively recharged from local precipitation while the older date for headwater sections suggests a more fossil groundwater source and lack of contemporary recharge. The ^{18}O similarity between groundwater in the mid-valley and the regional meteoric water line (MWL) suggests a Pacific moisture source and the role of El Niño precipitation in recharging local aquifers. Thus, El Niños and Pacific-sourced moisture are an important component of the regional hydroclimatology and the variation in ENSO frequency and intensity has significant social and hydrologic repercussions in these hyper-arid settings.

1. Introduction

The Atacama Desert, one of the driest regions on Earth, has an average annual precipitation of ~20–50 mm yr^{-1} which varies markedly both spatially and temporally (cf. Houston and Hartley, 2003). This region has experienced significant climatic changes over contemporary, Quaternary, and geologic timescales where the development of hyper-aridity during the Mid-to-Late Tertiary has been punctuated by drier and wetter periods over timescales of 10^1–10^3 years and where the effects of the El Niño-Southern Oscillation (ENSO) have been climatically profound throughout the Holocene and longer (Keefer et al., 1998; Magilligan and Goldstein, 2001; Keefer et al., 2003). Despite these extreme climatic conditions, this region has been an important environmental setting for sophisticated cultural development through

* Corresponding author.
E-mail address: Magilligan@dartmouth.edu (F.J. Magilligan).

0169-555X/$ – see front matter © 2008 Elsevier B.V. All rights reserved.
doi:10.1016/j.geomorph.2008.05.025

intensive and extensive irrigated agriculture and other cultural adaptations such as terracing and raised fields in highland or riverine settings (Dillehay and Kolata, 2004; Diaz and Stahle, 2007).

Several current debates remain about climate change in the Atacama Desert and across the Altiplano including the causes and timing of the onset of hyper-aridity during the Tertiary (Hartley and Chong, 2002; Dunai et al., 2005; Ewing et al., 2006; Clarke, 2006; Rech et al., 2006); the timing of the onset of ENSOs during the Holocene (Sandweiss et al., 1996; DeVries et al., 1997; Wells and Noller, 1997; Gomez et al., 2004); the magnitude and direction of precipitation anomalies during the Mid-Holocene (Grosjean et al., 2003; Rech et al., 2003); the identification of moisture sources and broader regional teleconnections (Cobb et al., 2003; Marchant and Hooghiemstra, 2004; Donnelly and Woodruff, 2007; Russell and Johnson, 2007); and, lastly, precipitation patterns across the Altiplano and Atacama Desert and their associated links to contemporary and Quaternary atmospheric circulation (Vuille et al., 2000a,b; Garreaud et al., 2003; Marchant and Hooghiemstra, 2004). Because of the strong topographic control of the Andes and their extensive latitudinal range, climatic variation is quite pronounced along coastal South America where the trade winds, the sub-tropical high pressure cell (STHP), and the westerlies all exist as possible circulation regimes and where considerable variation in precipitation exists.

The extreme climatic conditions in this geographic setting are exacerbated by the occurrence of El Niños and La Niñas. Significant flooding across the Atacama and Peruvian coastal deserts and droughts in the Andean highlands and Altiplano are linked to the magnitude of the El Niño-Southern Oscillation (the pressure difference between Darwin, Australia and Tahiti). The Atacama Desert lies in a latitudinal belt from ~°15 S to °25 S on the western side of the Andes, and its hyper-aridity is controlled by the rainshadow effect of the Andes which limits the transfer of moisture from the Atlantic Ocean trade winds westward across the topographic high of the Andes. This orographic effect is further compounded by the position and strength of the Pacific cell of the STHP that, in concert with the normally cool waters off the eastern Pacific, establishes an inversion layer of ~800 m on the western side of the Andes ultimately blocking eastward transfer of Pacific-sourced moisture. Moreover, the relative strength and position of the upper-level Bolivian High also modulates precipitation amount across the Altiplano (Lenters and Cook, 1997, 1999; Vuille, 1999; Vuille et al., 2000b; Garreaud, 1999; Garreaud and Aceituno, 2001; Garreaud et al., 2003). During El Niño years, the Pacific STHP weakens and trade winds diminish, which limit the upwelling of deep cool water off the eastern Pacific and ultimately allow rainfall on the arid western slopes of the Andes and dryer conditions across the normally wetter Altiplano (Fig. 1A), and disrupting most agricultural and cultural systems. At the other extreme of ENSO, strengthened La Niña's permit wetter conditions to prevail across the Altiplano but maintain dry conditions across the Andean western slopes, exacerbating normal patterns (Fig. 1B).

Although these atmospheric regimes are known to influence precipitation across the Altiplano and Atacama Desert, the links to the direction and magnitude of climate change and subsequent flooding are less well documented. Over the past several decades, researchers have investigated long-term regional proxies of climatic variability across the Central Andes, but most of these records come primarily from two distinct sources: (1) lake levels from Lake Titicaca (Abbott et al., 1997a, 2003) and other regional lakes (Abbott et al., 1997b; Placzek et al., 2006), and (2) isotopic signatures in the Quelccaya Ice Cap (Thompson et al., 1985). Although these records are temporally extensive, the tremendous topographic variability across the Andes limits their spatial application, and these localized proxy records may not have broad regional extent (Placzek et al., 2001). Despite the extensive literature on climatic and atmospheric circulation patterns, minimal focus exists on developing long-term flood chronologies across the Atacama Desert. Most of the previous work on paleofloods comes from Peruvian coastal regions (Wells, 1987, 1990; Keefer et al., 1998; Fontugne et al., 1999; Sandweiss et al., 2001; Keefer et al., 2003; deFrance and Keefer, 2005) with Andean proximal watersheds receiving far less attention, except for high elevation watersheds in Ecuador or Bolivia (Rodbell et al., 1999; Maas et al., 2001). These inland locations are perfectly situated to capture ENSO signals: the mainstem hydrology of the larger watersheds is broadly controlled by both El Niños and La Niñas and are, thus, sensitive indicators of the spatial variation of the occurrence of these two extreme circulation types. On the other hand, mid-elevation (~1000–2000 masl) ephemeral tributaries respond solely to localized precipitation that only occurs during El Niños. Thus it is possible to ascertain the occurrences of both ENSO indicators by examining alluvial chronologies for mainstem and tributary sections. Moreover, the significant presence of prehistoric agrarian village and state settlement in these oasis valleys provides an important additional proxy for flood chronology, as well as an important case study of the cultural management of flood risk by societies at several levels of social complexity.

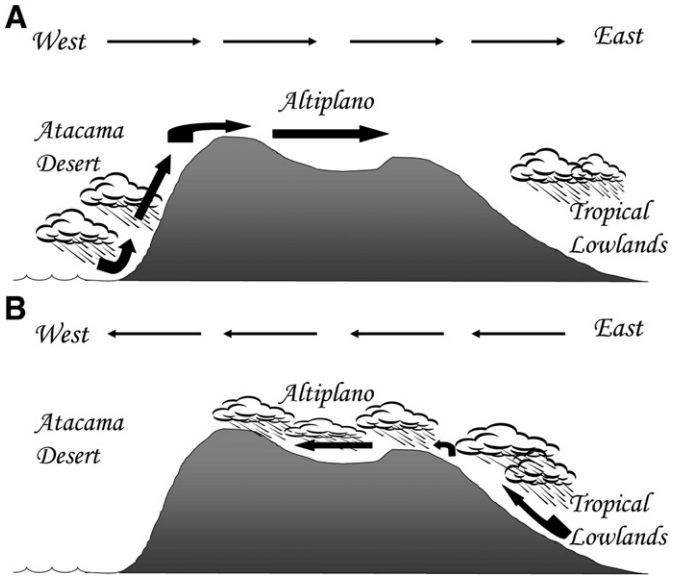

Fig. 1. General characterization of rainfall patterns across the Andes and Altiplano during pronounced (A) El Niño and (B) La Niña years. (Modified from Garreaud et al., 2003).

In this paper we focus on geomorphic and stratigraphic evidence of large floods in the Moquegua Valley to reconstruct hydrologic variation in the northern fringes of the Atacama Desert, Peru, and to link the magnitude and timing of these floods to established climatic records during the Late Quaternary. Lastly, other goals of this research are to determine the variations in La Niña and El Niño episodes to evaluate the relative importance of these coupled oceanic–atmospheric systems in controlling regional hydroclimatology and to determine the regional extent of these ENSO extremes. In this way, it becomes possible to establish whether Atlantic-sourced La Niñas drive precipitation or locally derived Pacific-sourced moisture during El Niños dictate hydrologic characteristics across these northern sections of the Atacama Desert.

2. Geomorphic, geologic, and climatic setting

We focus on the Rio Moquegua mainstem, a section of the Rio Osmore drainage that originates from the confluence of the Tumilaca, Torata and Huaracane Rivers downstream of the city of Moquegua (Fig. 2, 17.1956 S, 70.9353 W, 1534 masl), with a combined drainage area at the confluence of ~1600 km^2. Lacking any additional inflow from perennial tributaries, the Rio Moquegua mainstem flows for an additional 20 km in a continuous alluvial section before heading into a deep bedrock gorge immediately downstream of the archaeological

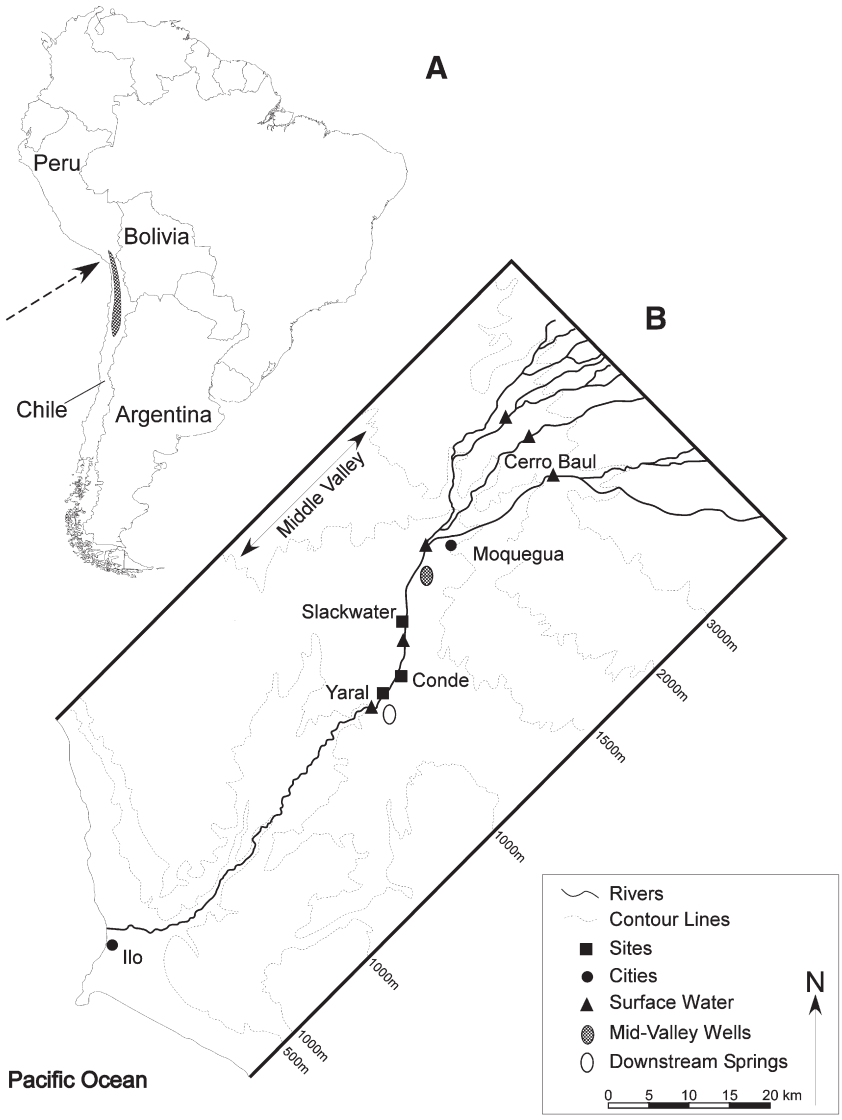

Fig. 2. Location maps of the Rio Moquegua. (A) Map of South America. Shaded area refers to core of the Atacama Desert, and the dashed arrow points to the mouth of the Moquegua (Osmore) River near Ilo, Peru. (B) Generalized location map with contours of main field area. Field work occurred primarily in a 20 km section of the mid-valley between the city of Moquegua and the site at Yaral.

site at El Yaral. Valley width ranges from 400–600 m in the study reach and reach gradient is 1.8%. The dominant lithology in the basin is the Moquegua Formation, a thick continental sedimentary sequence deposited during the Eocene and Oligocene (Marocco and Noblet, 1990): the Lower Moquegua Formation consists primarily of fine claystones and siltsones deposited unconformably across a well-developed erosional surface while the Upper Formation consists of Late Oligocene and Early Miocene volcanoclastics interbedded with siltstones and conglomerates.

The development of hyper-aridity in the basin is strongly tied to the uplift history of the Andes, one of the greatest topographic barriers to sources of moisture (cf. Rech et al., 2006). The Andean uplift history is neither uncomplicated nor resolved (Gregory-Wodzicki, 2000). The rapid uplift of the Andes during the Tertiary significantly influenced climatic and atmospheric conditions in the Central Andes that generated an extraordinary climate change – the shift to hyper-aridity – and that still influences the contemporary variation of precipitation. Early interpretations (Alpers and Brimhall, 1988) suggest a Mid-Miocene age for the development of hyper-aridity while recent evidence suggests that it is much younger, possibly Oligocene (Dunai et al., 2005) or even as recently as the Pliocene (Hartley et al., 2005), but most evidence points to an Oligocene–Miocene age for the generation of hyper-aridity (Rech et al., 2006). On contemporary timescales, the presence of the Andes has significantly affected atmospheric regimes and the magnitude and variation of incoming solar radiation that controls the location and magnitude of convectionally induced uplift, and, thus, rainfall amounts, across the Altiplano (Rowe et al., 2002; Placzek et al., 2006). This has further affected the penetration of Atlantic-sourced moisture and cut off the western side of the Andes from the trade winds, although it is uncertain as to how far down the west side this effect continues. Using modern precipitation records, Houston and Hartley (2003) have shown that precipitation gradients vary widely across the Altiplano with a pronounced difference in orographic precipitation on the eastern and western sides of the Andes. On the Peruvian west side between °15 S and °17 S they show that the mean annual rainfall (MAR, in cm) increases exponentially with elevation ($MAR = 4.7\ e^{0.0012A}$; where A is elevation in m), whereas on the eastside of the Andes the relationship is more complicated because of the long distances from the Atlantic and the variation in topography. Long-term climate records for the core region of the Atacama Desert (between °18 and °22 S) show, however, that zonal precipitation

decreases slightly with distance from the Atlantic, then increases at ˚64 W as the orographic effect of the Andes, in combination with increased convection, leads to the precipitation peak. Because of its distal location from the source, the isotopic composition of precipitation is extremely depleted in $\delta^{18}O$, with values generally between −25 and −30‰ across the high elevations of the western Altiplano (Aravena et al., 1999).

This longitudinal variation in precipitation is significantly linked to the timing and magnitude of ENSOs and thus flooding in the Atacama Desert. Precipitation across the Altiplano is enhanced during La Niñas when the associated Bolivian High shifts northward and intensifies thus enhancing the advection of moisture-laden air masses from the tropical Atlantic. The opposite occurs during El Niño when the Bolivian High weakens and shifts southward and diminishes rainfall totals across the Altiplano while the Atacama Desert receives maximum precipitation and flooding probability increases. Flooding on the mainstem Rio Moquegua reflects either localized precipitation during El Niños or the enhanced wetness across the high elevations of the Altiplano. Using aerial photography taken over the past 60 years. Manners et al. (2007) demonstrated that periods of major channel widening along the mainstem Rio Moquegua can occur during La Niña episodes as well as during El Niños, with disastrous consequences for floodplain agriculturalists. Ephemeral tributaries, however, can only flow and flood during local west side precipitation and this occurs only during El Niños.

This hyper-aridity, though, has been punctuated by wetter conditions regionally across the Altiplano and the Atacama Desert, especially during the Late Pleistocene, as these different circulation regimes have changed in position and intensity. Most research points to wetter conditions in the Atacama Desert and across the Altiplano during the Late Pleistocene, with mean annual precipitation increasing in some high elevation areas by as much as 100% compared to modern precipitation, associated with increased ENSO activity between ~17,520 and 16,270 cal yr BP (Betancourt et al., 2000; Latorre et al., 2006). Based on macrofossils in rodent middens within the canyon of the Rio Saluda in northern Chile (~2900 to 3200 masl), Latorre et al. (2006) identify more pluvial periods from 11,770–9550 cal yr BP, 7330–6720 cal yr BP, 3490–2320 cal yr BP, and at 800 cal yr BP. Their midden record suggests drier periods at 14,180 cal yr BP, 8910–8640 cal yr BP, and at 4865 cal yr BP. Late Holocene records from lake levels in Lake Titicaca suggest more arid conditions across the Altiplano from 2900–2800 cal yr BP, 2400–2200 cal yr BP, 2000–1700 cal yr BP, and 900–500 cal yr BP (Abbott et al., 1997a,b).

All ancient and modern land use in the Moquegua Valley depended on canal-fed irrigation. Irrigation systems can usefully be divided between relatively simple, but limited, floodplain agriculture and the amplification of irrigation through extended canals or terracing to reclaim more distant desert lands. Simple floodplain irrigation has been going on for millennia and may precede the beginning of an indigenous ceramic tradition in the Moquegua Valley, known as Huaracane (385 cal BCE–340 cal AD). Huaracane settlement and subsistence patterns suggest a generalist agrarian subsistence strategy and a low level of political and economic centralization (Goldstein 2000a, 2005). Huaracane domestic occupation in the Moquegua Valley was found at 169 habitation components totalling 73.5 ha in residential area, with all but five domestic components under 2 ha in size. Huaracane habitations were found on virtually every hilltop or slope along the rim of the valley bottom in the study area, at an average elevation only 48 m above the river level. This close relation to the floodplain indicates a reliance on simple valley-bottom canals. This distinguishes Huaracane's agrarian strategy from those of subsequent, politically more complex societies, notably the Tiwanaku state colonization of the region (ca. 600–1000 AD). Unlike the Huaracane pattern, Tiwanaku's large settlement enclaves were established far from the valley floodplain and associated with the reclamation of desert pampas through extensive canals and, of particular interest here, supplementary sources of ground water (Goldstein 2003, 2005; Williams, 2002). The Tiwanaku settlement and agrarian strategy represents agricultural intensification geared for surplus maize production for export to population centers in the Bolivian Altiplano (Hastorf et al., 2006). This indicates not only increased labor investment and coordination, and a fundamentally different cultural system, but the opening of a new economic "niche" dependent in part on real or perceived enhanced water availability at the major springs in the mid-valley. Following the Tiwanaku collapse, most of their extended irrigation systems were abandoned in the middle valley, and through the Inca, Spanish Colonial, and historic period, agriculture again retracted to the highly fertile valley-bottom lands.

3. Methods

3.1. Field procedures

The flood history program was conceived as an integral component of the Moquegua Archaeological Survey (MAS), a multi-year intensive survey of settlement history in the middle Moquegua Valley. This program began with a full-coverage pedestrian archaeological survey of the middle Moquegua valley (1993–1996) that documented over 450 settlement, mortuary or other components, primarily dating to the Formative, Middle Horizon, Late Intermediate and Inca periods. A second phase of site investigation research is ongoing since 1998, with intensive surface mapping, systematic collection and household and mortuary excavations at ten sites of various temporal and cultural affiliations in the survey area (Goldstein 2000b, 2005). Themes of particular interest are the advent of small scale Formative agrarian societies in the first millennium BCE, their increasing complexity and relations with other regions, their replacement by large enclave colonies of both the Tiwanaku and Wari expansive states in the Middle Horizon (ca. 500–1000 AD), the Tiwanaku and Wari collapse, and the rise and fall of smaller-scale local polities prior to the rise of the Inca in the 14th century.

Paleoflood data were derived from various sources but consist primarily of geomorphic and stratigraphic data collected over the past decade during five field excursions to the Rio Moquegua. These field data were augmented with aerial photography, remote sensing image analysis, and GPS mapping. For the field component, teams walked both sides of the ~20 km mainstem valley seeking evidence of paleofloods including flood gravels, slackwater deposits, cut-and-fill sequences, etc. A similar approach was used for tributary sections. In instances where datable material was found, each stratigraphic section was described, photographed, and its position was determined by GPS. Dating consisted of radiocarbon (^{14}C) dating of wood, charcoal and organic sediments and all samples were processed by Beta Analytic, Inc. In instances where the ^{14}C age intercepts the calibration curve at multiple dates, we determined the median calibrated age using the online version of CALIB 5.0 (Stuiver and Reimer, 1993) although this only occurred for a few younger dates generally <200 ^{14}C years BP. Because of the hyper-aridity, buried wood rarely exists stratigraphically although it sporadically occurs in tributary sections in part because many of these flood units were probably debris flows with the wood rafting on the flow surface during sediment transport. For mainstem exposures, organic lenses and paleosols were sampled for organic material. Because of limited precipitation, humate leaching to lower horizons is less of a problem thus minimizing contamination. Groundwater samples were collected in 2007 for radiocarbon dating. Samples were collected in 1 liter Nalgene bottles, and after collection, 2–3 pellets of NaOH were placed in each container to limit atmospheric exchange. The sites for groundwater sampling occurred primarily in the mid-valley on the southeastern flanks of the watershed although one site, Cerro Baul, exists in the highlands at ~2400 masl.

During the summers of 2006 and 2007, sediment samples were collected for dating by Optically Stimulated Luminescence (OSL). A 20 cm long, 5 cm diameter PVC pipe was pounded into the stratigraphic

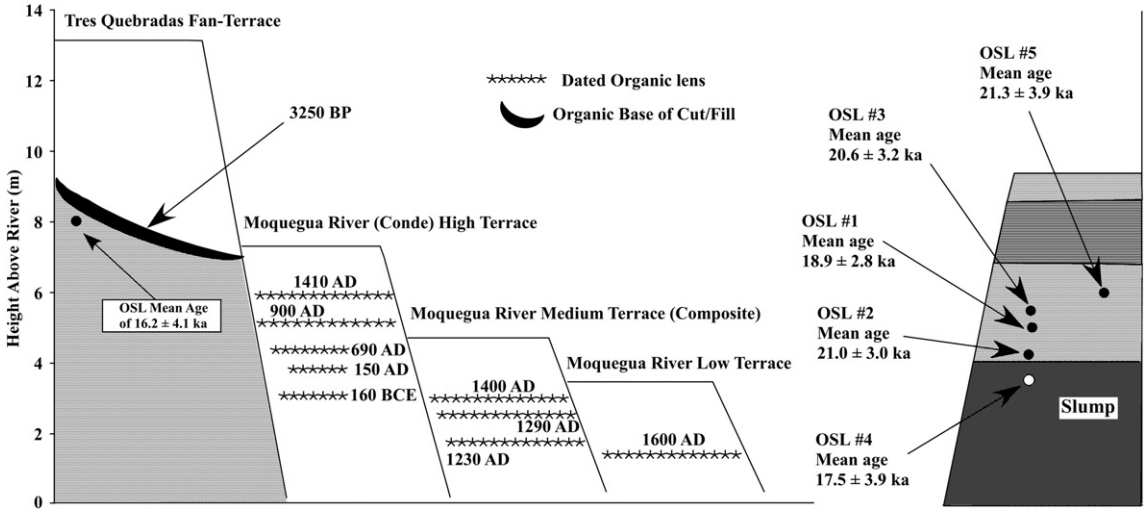

Fig. 3. Terrace heights (m) above the modern water surface along the mid-valley of the Rio Moquegua. The Tres Quebradas and the Slackwater Site are fan terraces while the remaining surfaces are mainstem alluvial terraces. For each terrace surface, the elevation of dated organic sediments is shown. The Slackwater and Tres Quebradas sites also have additional OSL dates.

unit and immediately wrapped in duct tape and placed in an opaque sampling bag to prevent any exposure to sunlight. Samples were submitted to University of Georgia Center for Applied Isotope Studies. For a complete description of their lab procedures, see Leigh et al. (2004).

3.2. Lab procedures

Sediment samples at key sites were further analyzed for particle size, organic matter content, trace elements, and clay mineralogy. For quantitative XRD (X-ray diffraction) analysis, samples were wet sieved to obtain the <2 mm fraction and then oven dried at 60 °C for 12 h. This sample fraction (3.6 g) was then combined with zinc oxide (ZnO) (0.4 g) and distilled water (10–15 mL) and micronized in a McCrone mill for 12 min to achieve a slurry of <10 μm particles. Randomly oriented powders were then prepared for XRD analysis in accordance with the spray drying technique outlined by Hillier (1999). Spray dried powders were then mounted on zero background plastic/epoxy slides and analyzed using a Siemens D-500 X-ray diffractometer operating at 40 kV and 40 mA with 0.05°2θ steps, 2 second counts, and CuKα radiation at the Clay Mineralogy Lab at Middlebury College. Peak intensities for quantitative analysis were determined using Jade® software (www.mdi.com) with an approach similar to Srodon et al. (2001). All XRD peaks and mineral intensity factors (MIFs) relative to ZnO are identical to those presented by Fisher and Ryan (2006). Distributions of sediment grain size were measured at the Marine Geology Lab at Middlebury College using a Horiba LA-920 Laser Particle Size Analyzer after being wet sieved into the <2 mm size fraction and undergoing ultrasonic disaggregation using Calgon® deflocculating powder. Organic matter was determined using the loss-on-ignition method; samples were burned in a muffle furnace for 6 h at 475 °C and the percent organic matter reflects the difference in weight post-oxidation. ^{210}Pb activities were determined using a high purity Germanium detector housed at Dartmouth College (see Magilligan et al. (2006) and Salant et al. (2007) for detailed lab procedures for determining total and excess ^{210}Pb activities).

Acidified samples were analyzed directly by inductively coupled plasma-optical emission spectroscopy (ICP-OES) on a Thermo Intrepid II for the following elements: Al, As, Be, Bi, Ca, Cd, Co, Cr, Cu, Fe, K, Li, Mg, Mn, Na, Ni, P, Pb, S, Si, Sr, and Zn. Quantification was based on comparison to a three point standard curve for a standard containing all elements, which typically afforded 3–4 orders of magnitude linear range in quantification. Concentrations were blank corrected by subtracting the concentration of a deionized water blank from the measured concentrations. Typical errors were <5% for most elements and all reported data are well above detection limits. The concentrations of major cations were determined following dilution in 0.1 N HNO_3.

The concentration and isotopic composition (δ^{13}C) of dissolved inorganic carbon (DIC), and the isotopic (δ^{18}O and δD) composition of water were determined to better characterize groundwater sources. DIC concentration and isotopic composition were measured sequentially on a Finnigan Delta XL+ isotope ratio mass spectrometer (IRMS) with GasBench automated inlet system. DIC is extracted from water as $CO_{2(g)}$ using concentrated H_3PO_4 in sealed, helium-flushed reaction tubes. After analysis, tubes are flushed to remove residual CO_2. Concentrations in each case are determined using peak intensities referenced to linear calibration from external standards. Isotopic composition is determined by reference to in-house standards and cross-calibration to accepted international values. Parallel analyses of standard reference materials (NBS18 and NBS19) were used to validate all procedures. Water isotopic compositions were measured using the Finnigan Delta XL+ IRMS in conjunction with a temperature conversion/elemental analyzer (TC/EA) and H-device.

Remote sensing was used to obtain elevation across the valley bottom for the 20 km section of the valley from the confluence of the Tumilaca, Torata and Huaracane Rivers to a downstream section where the river enters a bedrock gorge. We converted a 2003 ASTER image of the floodplain and adjacent areas to a 30 m ASTER-based DEM. From the DEM, 2 m contours were overlaid in ENVI® and exported as a shapefile to ArcMap. In this way, floodplain elevations were determined and ultimately contoured as heights above the channel bed in 2 m contours (cf. Manners et al., 2007).

4. Results

Based on a DEM compiled from an ASTER image, the 20 km stretch of the Rio Moquegua has a gradient of 1.8% throughout, lacks any recognizable knickpoints (Manners et al., 2007), and has several terrace surfaces that are irregularly scattered throughout the reach from ~2–18 m above the current water surface (Fig. 3). These terraces represent a range of fluvial terraces, fan terraces, or a combination of both.

4.1. Stratigraphy, composition and age of fluvial surfaces

The most detailed exposure comes from the Conde High Terrace site (17°19'24.7″S, 70° 59'23.1″W) which has five radiocarbon dates

Table 1
Radiocarbon dates for both mainstem and tributary sections and from groundwater sources

Site ID	Beta #	Conventional RC age (BP)	Error	Intercept with calibration curve (cal yr AD or BP)	1-sigma calibrated age	Material
A. Sites from ephemeral channels						
1. Rio Muerto						
Spring channel: Upper gray unit (1)	124116	620	±40	1350 AD	1300–1400 cal AD	Wood
Spring channel: Upper gray unit (2)	142835	730	±60	1270 AD	1255–1295 cal AD	Wood
Spring channel: Lower pink unit	124115	1290	±50	730 AD	670–775 cal AD	Wood
Geoprofile site: Middle Unit (below ash)	142834	620	±70	1350 AD	1290–1410 cal AD	Wood
Geoprofile site: Surface unit	222175	250	±50	1650 AD	1640–1660 cal AD	Wood
Lower Rio Muerto (1998)	133794	750	±60	1260 AD	1235–1290 cal AD	Wood
Lower Rio Muerto: Left Fork(A)	233983	2130	±40	2120 BP	2150–2050 cal BP	Wood
Lower Rio Muerto: Site X; S#1	233982	670	±40	1290 AD	1280–1380 cal AD	Wood
Lower Rio Muerto: Site Y; S#1	236883	640	±40	1370, 1380, 1390 AD	1280–1400 cal AD	Wood
Lower Rio Muerto: Site1 (Unit 5@65 cm)	222174	4820	±50	5590 BP	5600–5480 cal BP	Wood
Downstream Rio Muerto: Lower unit;S#2	233985	10,360	±60	12,150 BP	12,390–12,050 cal BP	Wood
Downstream Rio Muerto: Lower unit;S#1	241504	10,280	±60	12,060 BP	12,160–11,860 cal BP	Wood
Downstream Rio Muerto: Upper unit (45 cm)	236882	10,910	±60	12,870 BP	12,920–12,840 cal BP	Wood
2. Trapiche Fan						
Site A1	180013	190	±30	1670, 1780, 1800 AD	1660–1950 cal AD	Wood
Site D1	189090	140	±30	1680, 1730, 1810, 1930, 1950 AD	1680–1950 cal AD	Wood
3. Quebrada San Antonio	180012	370	±30	1490 AD	1460–1520 cal AD	Wood
B. Sites from the mainstem Rio Moquegua						
1. Conde High Terrace						
2003 Sample	189086	550	±40	1410 AD	1400–1420 cal AD	Organic sediment.
Sample A (2006?)	180008	1130	±70	900 AD	810–990 cal AD	Organic sediment.
S#1_2006 (283–295 cm)	220276	1310	±40	690 AD	670–760 cal AD	Organic sediment.
S#2_2006_317–327	222172	1840	±40	150 AD	120–230 cal AD	Organic sediment.
S#3_2006_362–380	222173	2110	±40	2110 BP	2140–2010 cal BP	Organic sediment.
2. Other Sites						
Pan American Highway: Sample 2	189089	60	±30	1950 AD	1890–1950 cal AD	Organic sediment.
Pan American Highway: Sample 1	189088	190	±60	1670, 1780, 1800 AD	1650–1950 cal AD	Charred material
Cutbank near Tres Quebrada (RB)	122794	320	±60		1485–1655 cal AD	Charcoal
Cutbank base upstream of Tres Quebrada	180015	580	±50	1400 AD	1310–1420 cal AD	Organic sediment.
Barking Dog Site (Sample#2)	203340	700	±50	1290 AD	1270–1300 cal AD	Organic sediment.
Barking Dog Site (Sample#1)	203339	820	±50	1230 AD	1180–1270 cal AD	Organic sediment.
Tres Quebrada Fan	180009	3250	±70	3460 BP	3560–3390 cal BP	Organic sediment.
Yaral (#1)	229542	3810	±40	4230, 4200, 4160 BP	4250–4150 cal BP	Organic sediment.
Across from Conde (RB-LT)	189087	Modern		Modern	Modern	Modern
Los Espejos flood gravel	180011	140	±50	1680, 1730, 1810, 1930, 1950 cal AD	1670–1950 cal AD	Charred material
Los Espejos burnt layer	180010	Modern	N/A	Modern	Modern	Organic sediment
C. Groundwater samples						
Zapata Well	234122	710	±40	N/A	N/A	Water
Cerro Baul Spring	234127	10,320	±40	N/A	N/A	Water
Pterodactyl Site	234126	3100	±40	N/A	N/A	Water

(Table 1), one OSL date, and also possesses a thin ash unit ~1.1 m below the surface that we interpret to be the Huaynaputina ash from 1600 AD (Thouret et al., 1999; Thouret et al., 2002). This terrace is ~7 m above the contemporary water surface and has a well-dated sequence of flood gravels, paleosols, and overbank deposits with a radiocarbon age of 2100 cal yr BP (160 cal yr BCE) for the lowest sampled flood unit 3.2 m above the current water level. Particle size analysis indicates that sand and silt dominate the matrix with generally less than 4–5% clay present although an upper and lower unit each have 7–8% clay. In general, a slight coarsening up sequence is present in the <2 mm matrix and in gravel–cobble size although sandier lenses occasionally exist at the base and in the upper, surface unit (Fig. 4). Organic matter content generally ranges between 2.5 and 3.5% with two important exceptions: a visible paleosol (900 cal yr AD) at 2.5–2.7 m having 6% organic matter and the contemporary surface layer having 8.5% organic matter.

Geochemically, the sediments consist primarily of plagioclase feldspar (mean=23.8%; standard deviation=4.2%) with correspondingly high quartz values present (mean=15.8%; standard deviation of 3.8%). Calcite exists irregularly in the profile limited primarily to the upper portion of the terrace generally between 0 and 2.8 m (Table 2) but is absent from 2.83–3.27 m, 3.62–3.88 m, and from 4.09–4.49 m. Clays are dominated by dioctahedral smectite with chlorite, kaolinite, and illite generally absent.

Several distinct flood deposits exist throughout the profile; they manifest specifically as gravel–cobble units or as a continuous package of undifferentiated gritty sands bounded distinctly from units above and below by texture or by color. These latter examples are suggestive of a single deposit and not continuous overbank deposition over time. We did not count units as individual floods in instances where neither distinct boundaries nor sedimentological breaks are evident. For our described section at the Conde High Terrace, we document 13 stratigraphically-recognizable major floods over at least 2100 cal yr BP with an average recurrence interval then of ~one extreme flood per 170 years. Flood frequency and magnitude, however, may have increased in the upper, younger section of the record. The overall matrix (<2 mm) reveals a coarsening upwards sequence (Figs. 4 and 5) and gravel and cobble clast size is generally larger in the upper portion of the profile. Two coarse gravelly units exist above the Huaynaputina ash with the one directly above it containing scattered large cobbles (Fig. 5). Four flood units are present between ca. 900 cal yr AD and cal 1410 AD (one flood per 100 years), generally within the time bracket of the Medieval Warm period, with the largest clast (*b*-axis=~100 cm) in a gritty–pebbly pink unit (unit 17 in Fig. 5) directly above the cal 1410 AD organic lens and below the 1600 AD ash. Two flood units occur between ca. 690 cal yr AD and 900 cal yr AD. These closely spaced floods bracket a period where fossil field furrows and ceramic

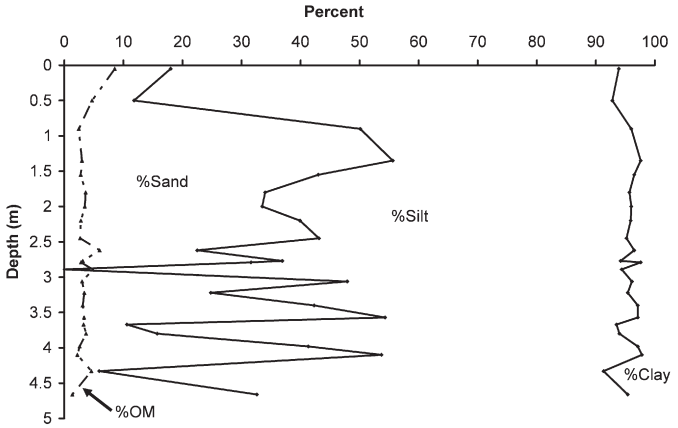

Fig. 4. Variation in texture (<2 mm) and organic matter with depth at the Conde High Terrace site along the mainstem Rio Moquegua.

sherds (Fig. 6) at Conde High Terrace indicate heightened agricultural activity under both the local Huaracane Formative culture and under Tiwanaku occupation. In contrast, only two flood units occur between ca. 150 cal yr AD and 690 cal yr AD (two per 540 years). Three stratigraphic units are present between 160 cal yr BCE and 150 cal AD but only two of them (units 6–7) represent distinct floods while one unit (unit 5) does not resemble a distinct flood; this time period thus has two large floods over ~840 years. No flood units occur below the cal 160 BCE silt unit. In a more northern, coastal location Wells (1990) similarly noted an increase in flood frequency during the Late Holocene with four large floods occurring between ca. 1250 BCE and ca. 1325 AD (one per 630 years) while nine floods occurred post ca. 1350 (one per 75 years).

A high fluvial terrace exists at the farthest downstream alluvial section, immediately before the river enters the bedrock gorge. This terrace location, called El Yaral (Fig. 2), is culturally rich with over 300 residential terraces located on adjacent steep hillslopes that contain two cemeteries and two communal buildings (Rice, 1993). This archaeologically important site represents one of the key agricultural and domestic sites of the post-Tiwanaku Chiribaya culture. This site was initially occupied ca. 1000 AD (Rice, 1993) but was abandoned following the catastrophic Miraflores flood of ca. 1330 AD, which has been documented throughout the Atacama Desert and the Pacific (Nunn, 2000; Kumar et al., 2006), with specifically catastrophic effects on certain coastal Chiribaya settlement sites (Wells, 1987, 1990; Magilligan and Goldstein, 2001; Keefer et al., 2003). This 9.8 m high terrace consists almost entirely of well rounded, large flood-derived boulders (Fig. 7), and organic material embedded within the lower gravels in this unit generated a ^{14}C date of 4200 cal yr BP (2σ=4390–4090 cal yr BP). The lithologic effect is manifest here; the valley is merely 310 m wide at this location and a choke point exists (locally called "Los Espejos" — the mirrors) immediately upstream that is only 45 m wide. This upstream constriction leads to high flow velocities as the entire discharge of the Rio Moquegua watershed passes through this choke point. The flow divergence immediately downstream at the Los Espejos choke point leads to sediment deposition of coarse boulders transported through the constriction. Using the size of the largest 10 particles (mean *b*-axis=2000 mm) and equations developed by Costa (1983), we estimated the discharge of this flood (Table 3). Velocity is estimated to be ~6.5 m/s and the mean flow depth is 4.9 m (Table 3). These boulders came primarily from the base of the unit ~2 m above the current stream bed. The combined flow depth (6.9 m above stream bed and still 3 m below the terrace surface) provides an extremely conservative estimate of ~13,000 m^3/s. Using the height of the terrace surface of 10 m and the full cross-valley width of 310 m yields an estimated discharge of ~20,000 m^3/s. For reference, Magilligan and Goldstein (2001) determined that the 1997–98 El Niño flood was ~450 m^3/s based on HEC-RAS modeling.

Several exposures exist of a surface approximately 4.5 m above the river bed that occurs throughout the Moquegua Valley. No geochemical or particle size data exist for this terrace but it has been radiocarbon dated at two sites: at Tres Quebradas and at Barking Dog. For the Barking Dog Site, the terrace surface is 4.34 m above the modern water surface with gravels exposed ~3.4 m below terrace top (0.9 m above modern water surface) but their elevation varies irregularly and these gravels appear to be the elevation of the paleo-point bar. Two organic lenses occur here: the lower one, dated to 1230 cal AD, is 2.45 m below the terrace top and the upper one, dated to 1290 cal AD, is 1.85 m below it. The stratigraphy lacks any flood gravels and consists primarily of brown silty material throughout the profile. This terrace seems to represent a site of continuous fine-grained overbank deposition post-1230 AD. Based on the calibrated date of the lower organic lens, this suggests that 245 cm of material accumulated since 1230 AD, generating a sedimentation rate of ~3 mm yr^{-1}. The medium terrace at Tres Quebradas is along the right bank exposed from significant channel erosion in 1998 (Manners et al., 2007). It is similarly fine-grained throughout and has a radiocarbon date on a basal black organic lens exposed ~3.5 below the surface top of 1400 cal AD.

The low terrace/floodplain surface is 2 m above the contemporary water surface and has frequent exposures of flood gravels. Radiocarbon dates on charcoal or organic lenses indicate relatively young dates on these units ranging from modern to mid-nineteenth century (Table 1). At the Pan Am Site, the lower date (at 67 cm below surface) comes from a poorly sorted gravel matrix that appears to represent the top of the point bar gravels. These gravels date to 190 ^{14}C years BP and although multiple intercepts occur with the calibration curve, the median calibrated age is ca. 1770 AD. The overlying gravels (60±30 ^{14}C years BP) have a median age of 1870 cal yr AD but may be younger because of dating uncertainties.

4.2. Alluvial chronologies in tributary sections

Evidence for Quaternary flooding in tributary sections is based on walking the banks of >10 ephemeral channels of the Rio Moquegua with more than 50 km of channel covered over 10 years. Unlike flood deposits of the mainstem, these are coarser and generally lacking in material <0.063 mm and further lacking organic sediment. Alluvial fills are generally 1–2.5 m high depending on the depth of local channel incision. Because these tributaries are near hillslope sediment sources, the deposits tend to be a mixture of fluid flows and debris flows (see typical stratigraphy in Fig. 8B and 8C). In some situations, because of the fluid rheology, wood is occasionally buoyed within, or on top of, the flow and trapped during deposition ultimately providing material for ^{14}C dating. Furthermore, many of these channels have well-developed fans at distal ends that exist as fan terraces (Tres Quebradas Site) if they extend into the mainstem valley, or as fresh cut faces where the mainstem has truncated the fan (Slackwater Site).

The most detailed and best dated sequence comes from a 14.5 km^2 watershed, Rio Muerto, situated immediately upstream of the Conde High Terrace (Fig. 8A). This is a well dissected catchment with multiple sub-drainages that head on the flanks of Pampa Lagunas, an extensive Mid-Miocene erosional surface (Tosdal et al., 1984). Four sections in the middle-to-lower 3 km had exposed datable material in flood deposits with absolute ages ranging from 250 cal yr AD to 5590 cal yr BP. Earlier, Magilligan and Goldstein (2001) reported flood deposits at the Spring Channel Site associated with the regionally extensive and catastrophic Miraflores flood of ca. 1330 AD and an earlier flood ca. 700 AD. New dates at the adjacent Geoprofile Site now reveal evidence of the Chuza flood, a catastrophic El Niño event associated with massive debris flows along the Peruvian coast (deFrance and Keefer, 2005). This deposit, ^{14}C dated to cal 1650 AD (Table 1), sits directly atop the Huaynaputina ash of 1600 AD (Fig. 8B) and is probably

Table 2
Results from quantitative XRD analysis

Sample ID	% Quartz	% Calcite	% Plagioclase feldspar	% Potassium feldspar	% Dioctahedral clay	% Trioctahedral clay	Total	Smectite
Conde20a@0.05	12.01	4.2	24.2	4.9	17.1	6.5	68.91	Likely
Conde20b@0.50	11.73	3.9	22.7	5	15.9	6.7	65.93	Likely
Conde19@0.90	10.33	1.5	24.6	6.1	12.2	5.9	60.63	Yes
Conde17@1.35	14.87	2.2	22.9	7.9	20.5	9.3	77.67	Likely
Conde16@1.55	11.44	1.7	25.6	5.5	12.7	10.9	67.84	Yes
Conde15@1.80	15.76	3.3	21.4	6.4	19	5.4	71.26	Yes
Conde14@2.00	14.76	2.7	24.8	5	16.1	6.9	70.26	Yes
Conde13a@2.20	11.52	2.6	25.2	5	15.3	9.8	69.42	Yes
Conde13b@2.45	12.99	2.1	21	5.6	16.8	6.3	64.79	Likely
Conde12@2.62	12.25	1.6	18.6	6	16.4	7.2	62.05	Likely
Conde11@2.77	12.01	1.2	17.4	4.4	14.4	8	57.41	Yes
Conde10@2.79	21.02	2.6	34.5	ND	23.2	11	92.32	Yes
Conde9c@2.89	19.67	ND	25.3	5.7	16.6	tr	67.27	Maybe
Conde9a@2.89	15.17	ND	20.5	ND	13.6	2.4	51.67	Likely
Conde8@3.06	18.25	ND	21.2	6.7	15.8	7	68.95	Yes
Conde7@3.22	15.27	ND	21.6	4.6	18.3	7.2	66.97	Yes
Conde6@3.40	15.39	1	25.9	3.4	12.5	8.3	66.49	Yes
Conde5@3.57	12.26	1	21.8	3.8	22.1	10.8	71.76	Yes
Conde4a@3.67	14.26	ND	22.4	3.2	22.4	3	65.26	Yes
Conde4b@3.80	15.78	ND	24.7	4.7	22.4	9.4	76.98	Yes
Conde4c@3.98	20.92	1	29.8	5.6	13.3	7.8	78.42	Likely
Conde3@4.10	18.79	ND	24.5	49.2	8.4	ND	100.89	Maybe
Conde2@4.33	12.41	ND	18.5	2.8	20.7	ND	54.41	Yes
Conde1@4.6	26.89	1	31.2	ND	8.9	8.9	76.89	Maybe

associated with the coarse sandy gravel unit atop the ash at the Conde High Terrace (Fig. 5). Four other flood units occur beneath the ash; a unit directly below the ash is dated at 1350 AD (Fig. 8B) and is probably the Miraflores flood while the lower three lack any material for dating. Two more dated sites exist several km downstream. Site 1 at Lower Rio Muerto contains evidence of four major floods/debris flows, with the lowest, coarsest unit dated to 5590 cal yr BP. Although none of the stratigraphically higher units are dated, alluvial material 50 m downstream on the right bank, probably associated with the Miraflores flood elsewhere in the valley, is dated at 1290 cal yr AD. Recent field work in 2007 at an adjacent site, ~200 m upstream, identified another alluvial sequence with datable material (Site Left Fork (A)) that reveals a debris flow deposit dated to 2120 cal yr BP (Table 1; Fig. 8B) with two younger alluvial units and five–six older units (Fig. 9). The last site in Rio Muerto (Downstream Rio Muerto) occurs at the most downstream location ~300 m directly east of the Pan American highway. This 4 m high terrace contains several debris flow units with unit below the surface layer dated to 12,870 cal yr BP and the immediately lower debris flow unit having two dates on separate pieces of wood of 12,150 and 12,060 cal yr B, respectively (Table 1), with three debris flow deposits below this lower dated unit (Fig. 9). Although the dates are not stratigraphically coherent (wood in upper dated unit is too old), the correspondence of dates between 12,060 and 12,870 cal yr BP suggests aggradation up to the approximate termination of the Younger Dryas.

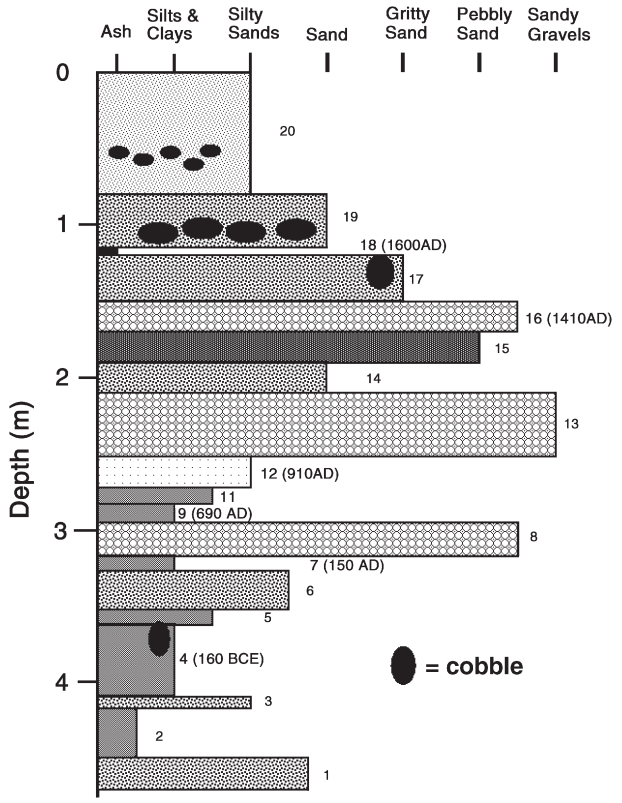

Fig. 5. Generalized stratigraphic column for matrix composition for the Conde High Terrace. Numbers adjacent to fills are the unit numbers based on field descriptions. Unit 10 is not in the profile and refers to the laminated silts in the in-filled irrigation canal.

The other tributary locations have significantly younger flood deposits than those at Rio Muerto (Table 1). Some of the units may be older but dates come from the highest stratigraphic unit. At the Trapiche Fan Site (Site A1) four flood units are recognized; with the upper unit containing material dated to cal 1680–1950 AD (the 1σ range is used here as the ^{14}C date has several intercepts with the calibrated curve although the median intercept age is 1770 cal yr AD). The upper, dated unit is the coarsest unit and because it is inversely graded and matrix-supported it is probably more of a debris flow. Evidence for historical El Niños comes from another catchment, Quebrada San Antonio, several km south of Trapiche. Again, the dated flood deposit comes from the upper unit and it has a ^{14}C date on a piece of wood that dates to 1390 cal yr AD (2σ=1450–1630 cal yr AD). This unit lies directly below the Huaynaputina ash and is probably an El Niño flood that occurred prior to the Chuza flood but some time soon after the Miraflores flood.

4.3. Flood stratigraphy in alluvial fans and fan terraces

Two well-dated alluvial fans occur within the mid-to-lower section of the main valley. The Tres Quebradas Fan is a fan terrace ~14–16 m above the current river level that contains a basal sequence of

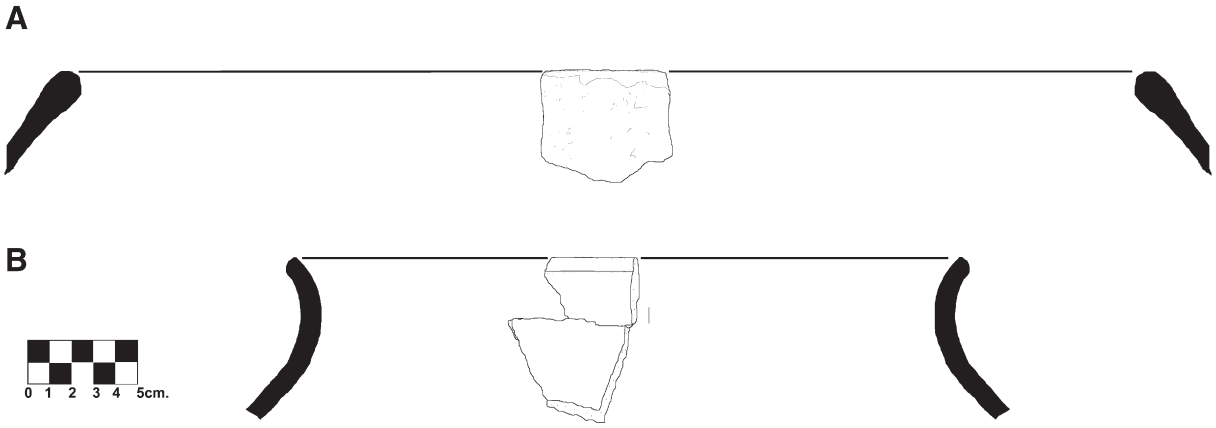

Fig. 6. Ceramic sherds associated with Conde High Terrace layer 9 (agricultural furrows): (A) Huaracane "neckless" olla (ca. 500 BCE–700 AD); (B) Tiwanaku plainware olla (ca. 600–1000 AD).

generally clast supported fine-to-medium gravels. One OSL date in a sandy lens, ~7 m below the terrace surface, dates to ~16 ka (Fig. 10). A cut-and-fill sequence, dated to 3250 cal yr BP by AMS, truncates these basal gravels with the fill material containing flood gravels and poorly sorted gravelly sands. The fill has a parabolic base and a similar geometry for the undated flood gravels with 1 m of yellowish brown silts separating the peaty organic base from the flood gravels. The basal stratigraphy suggests a pattern of more perennial flow in these Late Pleistocene fine-to-medium gravels. We interpret that more frequent flows occurred at this time because of the thick sequence (up to 4 m at the more proximal end of fan) of horizontally bedded clast supported gravels dating to ~16 ka. Units above these basal gravels are a finer matrix and are probably associated with a mixture of fan and mainstem alluvium.

Further upstream along the mainstem at the Slackwater site, the recent channel migration has truncated a right bank alluvial fan that is ~9–10 m above the modern river level. This stratigraphy contains a thick sequence of ~12 indurated sandy gravelly to gravelly sandy units interbedded with more matrix-supported beds that are probably up-fan debris flows. These 12 units are generally laterally continuous across the fan face although small cut-and-fill sequences exist near the surface (Fig. 11). Although the five OSL dates do not sequentially reflect stratigraphic position (lowest date is 17.5 ka and upper unit is 21.3 ka), the consistent overlap (including error bars) of these fives dates indicates that most of the fan sequence dates to the Late Pleistocene and most likely the Late Glacial Maximum (Table 4). Furthermore, the upstream portion of the fan contains 2.3 m of laminated slackwater deposits with the Huaynaputina ash of 1600 AD at the base of the slackwater sediments. Mean particle size of these 27 units ranges from 25–900 mm with the nine beds between 7–8 and 8.5 m above the water surface being generally coarser than the immediately lower units, except for the first bed above the ash which is probably the Chuza flood recognized elsewhere in the valley (Fig. 12). Results from three samples representing the lower, middle, and upper portion of the slackwater sequence shows that these beds have higher quartz (~20%) and significantly lower potassium and plagioclase feldspar than

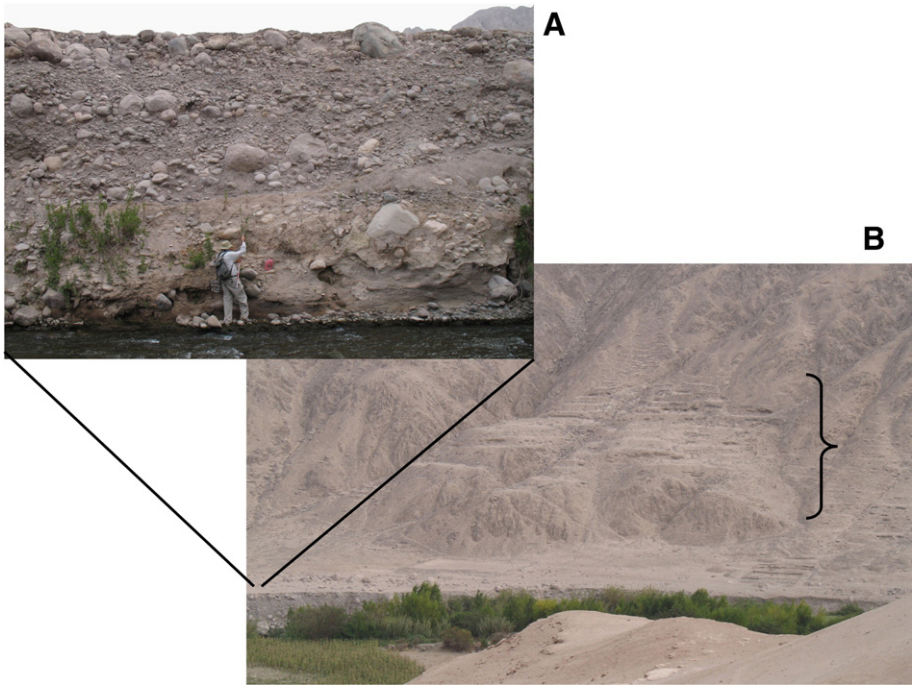

Fig. 7. El Yaral Site. (A) Flood gravels in high terrace and (B) view of alluvial terrace and hillside domestic terraces (shown by parenthesis).

Table 3
Paleoflood discharge estimates for the flood gravels at El Yaral (Fig. 7)

Hydraulic variable	Value
Mean particle size (mm)[a]	2000
Valley width (m)	310
Slope (m/m)	0.018
Velocity (m/s)[b]	6.35
Water depth above gravels (m)[c]	4.9
Total water depth	6.9
Minimum estimated discharge (m^3/s)	13,590
Estimated discharge using terrace top (m^3/s)	19,301

[a] Based on 10 largest particles.
[b] Based on Fig. 4 in Costa (1983) where $V=0.2d^{0.455}$.
[c] Based on Fig. 7 in Costa (1983) using slope and particle size.

potentially similar aged sediments at the Conde High Terrace. Because these sediments result from mainstem flooding, it is not possible to determine whether the floods associated with their deposition were either of El Niño or La Niña origin. Each of these units is dead in excess ^{210}Pb indicating that all units are older than ca. 1900 AD (~5 half-lives of ^{210}Pb where it completely decays). The unit is well constrained at the base but is only partially constrained at the surface, thus these slackwater sediments represent no more than 300 years of accumulation. Assuming it is 300 years, that would be one mainstem flood on average every 11 years, but because the upper unit lacks strong temporal control, it may represent more frequent flooding.

5. Discussion

5.1. Composite history of Late Pleistocene–Holocene floods

The climate of the Late Glacial Maximum (LGM) in the central Andes was generally wetter than at present. Some precipitation estimates of LGM precipitation are twice the modern in the high elevations of the Atacama Desert (Betancourt et al., 2000; Latorre et al., 2006), and the Altiplano is similarly wetter during the LGM in part because of the intensified trade winds advecting moisture from the Amazon Basin (Baker et al., 2001; Placzek et al., 2006). Little hydrologic evidence exists, however, for lower topographic positions more distal from the Andean crest and its orographic control on precipitation. Evidence from fans and fan terraces in the Moquegua Valley suggest that large floods occurred with a greater frequency during the Late Pleistocene and perhaps to the approximate termination of the Younger Dryas (ca. 12,000 cal yr BP). The Slackwater Site (Figs. 3 and 11) reveals a sequence of 12 floods of localized precipitation beginning by at least 20 ka. Several erosional unconformities and cut-and-fills occur in this sequence so the number of floods may be larger. The coarse gravel texture typical of these Pleistocene deposits is coarser than any of the Holocene units in the sequence. For the Tres Quebradas site, an OSL date indicates that the fan was quite active up to at least 16.2 ka (±4.1) and the sedimentology of these Pleistocene deposits suggests more perennial flow. Lastly, for the terrace surface at the most distal end of Rio Muerto, ^{14}C dates between 12,060 and 12,870 cal yr BP on upper debris flow deposits indicate that Late Pleistocene flooding essential ceases some time around the termination of the Younger Dryas. Stratigraphic evidence of Niño-derived floods does not emerge again until the end of the Mid-Holocene ca. 5.6 ka.

Determining the Mid-Holocene climate of the central Andes remains a contested topic. Based on an array of paleoclimatic evidence, Grosjean et al. (2001, 2003) suggest that the Atacama Desert may have been drier than at present during the Mid-Holocene which corresponds to low lake levels in Lake Titicaca (Cross et al., 2000). Their paleo-ecological evidence has been recently questioned, however, by several studies (cf. Betancourt et al., 2000; Holmgren et al., 2001) that contend that the Mid-Holocene may have been wetter in specific parts of the Atacama Desert. The lack of dates between ca. 5.6 ka and 12 ka in our ephemeral channels can result from either major channel erosion prior to 5.6 ka, buried deposits below contemporary bank levels, or a lack of bed mobilizing floods. Results presented herein suggest that large Niño-related floods did not occur in the Holocene prior to ca. 5.6 ka. These channels are on or near bedrock (or at least indurated gravels) although some lateral stripping of "floodplains" in these ephemeral channels may have occurred prior to 5.6 ka. Most stratigraphic evidence, however, suggests that limited Mid-Holocene El Niño flooding occurred in these mid-elevation west side channels, thus suggesting a drier climate during this interval. Our date for the start of the Early-to-Mid-Holocene cessation of El Niño flooding may be somewhat too old because we lack datable evidence of its termination. In a nearby coastal setting, Keefer et al. (2003) suggest the Early Holocene was the period of greatest activity and the Mid-Holocene hiatus of El Niño flooding lasted from ca. 8400 to 5300 cal yr BP.

5.2. La Niña vs. El Niño: hydrologic–geomorphic coupling

Because of the complex regional hydroclimatology of the central Andes, it is quite difficult to link specific floods to either extremes of ENSO. Previously, we demonstrated that 20th century floods along the mainstem Rio Moquegua can result from either La Niñas or El Niños (Magilligan and Goldstein, 2001; Manners et al., 2007). Therefore, flood stratigraphy within the mainstem valley is non-deterministic as either mechanism can spawn large floods. However, the ephemeral tributaries throughout the mid-valley can only flood during localized precipitation, which can only occur during El Niño episodes. This regional and watershed scale distinction provides the opportunity to separate out flood producing mechanisms and may provide an important proxy for regional climate, the timing of climatic shifts, and the direction of change.

Flooding along the mainstem Rio Moquegua has intensified during the past ~2 ka, and evidence in the most downstream section by Yaral indicates that perhaps the largest Late Holocene catastrophic flood occurred ca. 4200 cal yr BP (3810 ^{14}C years BP). We adduce the intensification of mainstem flooding to the increased number of flood deposits within the Conde High Terrace; the presence of a gritty–pebbly matrix in upper units, and the increase in gravel–cobble clast size in near-surface units (Fig. 13). The increased flooding during the Late Holocene corresponds to broader regional increases. For example, Wells (1990) also recognized increased flooding during the Late Holocene in northern, coastal Peru where four large floods occurred between ca. 1250 BCE and ca. 1325 AD, while nine floods have occurred since ca. 1350 AD. Similar results have been found in adjacent coastal and maritime settings (Sandweiss et al., 2001; Riedinger et al., 2002; Rein et al., 2004, 2005; Rein, 2007). Moreover, this Late Holocene intensification of floods is equally pronounced beyond the central Andean region. In a detailed lithostratigraphic and mineralogical analysis of sediments in Bainbridge Crater Lake in the Galápagos, Riedinger et al. (2002) show that the intensity of Niño-derived floods of strong-to-very-strong intensity increased dramatically in the past 3000 years. Of their 110 events of this intensity in the past 6100 years, 73% of them have occurred since 3 ka. They also note a significant absence of floods of either moderate or strong-to-very-strong intensity between 5000 and 4000 years BP.

The dual mechanisms for flooding prevent identification of specific El Niño episodes. In some instances, the radiocarbon dates correspond well between stratigraphic units in the ephemeral tributaries and in the mainstem. For example, a large debris flow ca. 2100 cal yr BP in Rio Muerto seems to correlate with a flood deposit at the base of the Conde High Terrace suggesting the occurrence of a regionally extensive large El Niño. This is also true of the historically documented Chuza event at 1607 AD which manifests stratigraphically in the mainstem Rio Moquegua at the Conde High terrace. This flood must have been associated with significantly elevated ENSO metrics (high sea surface temperatures, depressed Pacific STHP, and aridity in the Altiplano) because its effects were broadly felt throughout South

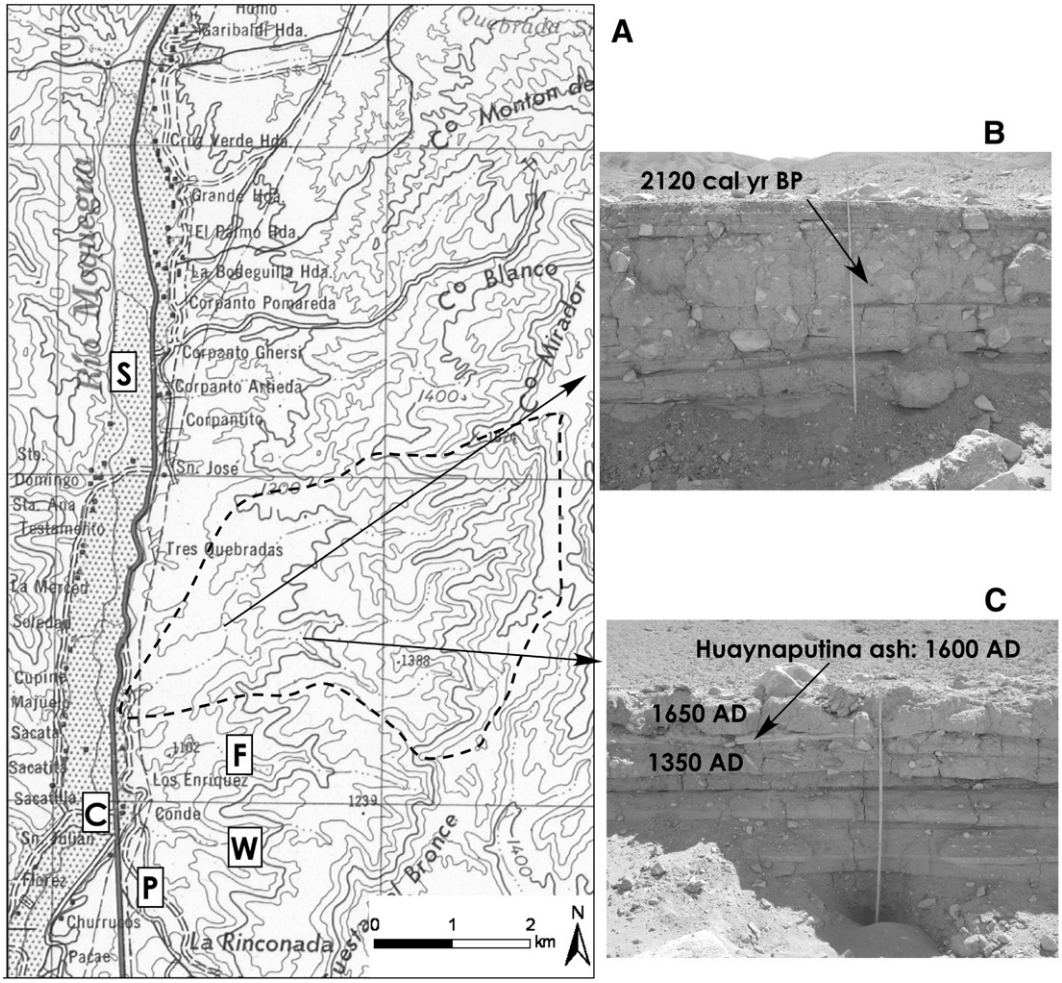

Fig. 8. (A) Topographic map of the lower section of the Rio Moquegua. Outline of the Rio Muerto tributary watershed shown in dashed line (watershed area is 14.5 km^2). Locations on topographic map are Conde High Terrace (C); Slackwater Site (S), Foxpath (F); White Ruins (W) and Pterodactyl (P). Upper picture (B) is a close-up of the dated stratigraphy at Lower Muerto (LF A) and the lower picture (C) is a close-up of the Geoprofile Site stratigraphy in the upper Rio Muerto with the Chuza Flood (ca. 1650 AD); the Huaynaputina ash (1600 AD), and the Miraflores Flood (ca. 1350 AD).

America (Meggers, 1994; Keefer et al., 2003) and the broader Pacific region including California (Schimmelmann et al., 1998, 2003).

Linking flood history to climate is always problematic as floods can occur during dry or wet periods, but the probability of floods occurring generally increases in wet periods (Knox, 2000). For the Moquegua Valley, the Mid-Holocene drought that was global in scope also manifested here and broadly across the Atacama Desert (Grosjean et al., 2001, 2003). It was associated with some of the lowest lake stands in Lake Titicaca (Seltzer et al., 1998) and suggests an in-phase relationship between the Altiplano and the Atacama Desert. This in-phase relationship can occur during wet phases as well, as seen by the frequent Late Pleistocene debris flow deposits at the Slackwater Site and the thick gravel sequences at the Tres Quebradas Site. Somewhat uncharacteristic of this in-phase relationship, though, is that wet periods on the Altiplano are generally associated with intensified La Niñas, normally corresponding to colder SST off the eastern Pacific (SST for the LGM have been estimated to between 3 °C (Gagan et al., 2004) and 4.5 °C (Peltier and Solheim, 2004) cooler than at present). This oceanic condition normally leads to droughts on the Andean west side slopes, especially at the elevations of the mid-valley of the Rio Moquegua (1000–1500 masl) (Garreaud and Battisti, 1999; Garreaud, 2000; Garreaud and Aceituno, 2001; Garreaud et al., 2003). These dates on fan gravel deposits suggest that advection of Pacific-sourced moisture must have been more common and perhaps more intense during the LGM to generate frequent flood gravel sequences within ephemeral channels, while at the same time the Altiplano was significantly wetter due to advection of Atlantic-sourced moisture. This dual wetness in the Atacama Desert and Altiplano at this time suggests that ENSO must have been more variable to permit filling of Lake Titicaca while simultaneously spawning periodic large El Niño floods in the Atacama Desert.

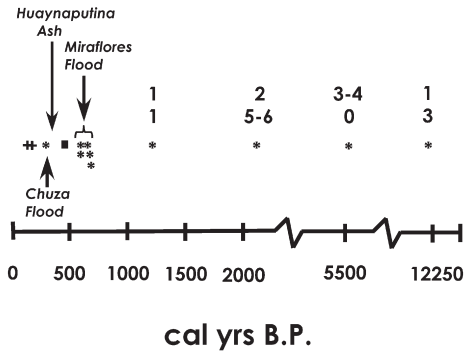

Fig. 9. Time series of dated flood deposits of (warm phase) El Niño origin. The association with El Niño exists because these flood deposits all occur in tributary valleys of the Rio Moquegua and lack direct connection to highland precipitation, typical of (cold phase) La Niña episodes. Dated units for the Rio Muerto are shown by asterisks while flood deposits for the Trapiche tributary are shown by plus signs. For the dated deposit along Quebrada San Antonio, it is shown as a solid square. The numbers above the symbols refer to the number of individual flood deposits occurring above (upper number) or below (lower number) the dated unit. Note the *x*-axis is punctuated and has two sections of non-continuous time.

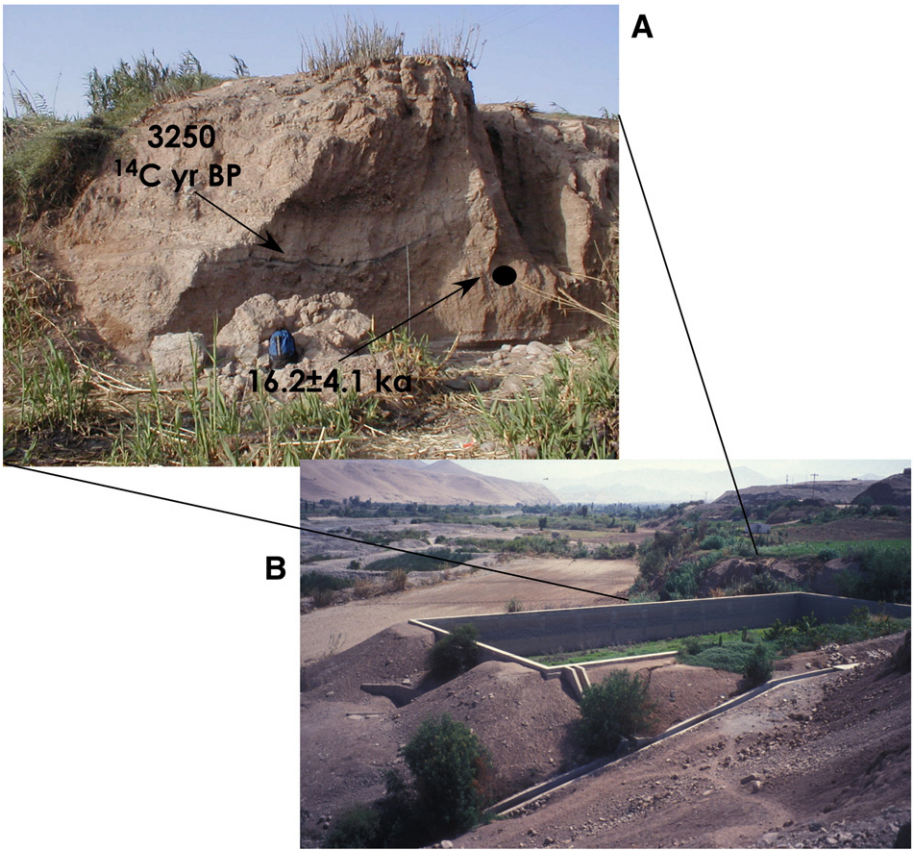

Fig. 10. Photos of the Tres Quebradas fan terrace. (A) Close-up of fan stratigraphy with dates, and (B) a view from Pan American Highway.

Although still not well known, recent modeling efforts also suggest that the ENSO signal may have been more variable during the LGM (An et al., 2004; Drost et al., 2007; Peltier and Solheim, 2004).

Unraveling the variation in ENSO is further complicated by the lack of older fluvial surfaces in the mid-valley Rio Moquegua. Although older terrace levels exist in the main valley, most of the alluvial surfaces in the mid-valley are generally less than 6 m above the modern water level. By correlating the elevation of these surfaces (compiled from the DEM from an ASTER image) with known radiocarbon ages, Manners et al. (2007) showed that more than 70% of the alluvial material is younger than ~600 ^{14}C years. This distribution of younger fill, shown in Fig. 14, indicates that most of the alluvial material is quite young and suggests that a major erosional episode occurred prior to ca. 600 ^{14}C years BP. Historical floods generate massive lateral channel erosion with up to 2–3 ha per river km commonly occurring during large floods (Magilligan and Goldstein 2001; Manners et al., 2007). The lack of cohesive banks and riparian vegetation combine to enhance lateral erosion which can occur by either la Niña or El Niño floods. The isolated older terrace remnants older than Late Holocene are thus rare in the mainstem valley and limit identification of older flood units.

5.3. Niños, NIÑOS, and MEGA-NIÑOS

The stratigraphic evidence and geo-chronological dating of these flood deposits suggest that large floods, some of them quite catastrophic, have occurred widely in these hyper-arid drainages of the Atacama Desert, and furthermore they have a strong correspondence to the El Niño-Southern Oscillation (ENSO). However, El Niño is an oceanic–atmospheric definition (Trenberth, 1997): it may differ significantly in its terrestrial impact, and not all atmospheric phenomena defined as an El Niño will have the same hydrologic impact across the Atacama or elsewhere. In some instances, the magnitude (and cultural impact) of El Niños in the pre-historical period is so large that they have been dubbed "mega-Niños" (Keefer et al., 2003).

In essence, El Niños are an unusual occurrence and most years lack the oceanic–atmospheric coupling that spawns these events. On contemporary timescales, meteorological observations such as the Southern Oscillation Index (SOI) demonstrate that El Niño occurs, on average, once every 7–8 years: a periodicity which seems to have been established by at least 5 ka (Rodbell et al., 1999). However, despite the relatively frequent occurrence of El Niños, not every El Niño has the same intensity (Quinn et al., 1987) nor do they generate the massive rainfall and flooding as occurred in 1997–98 and in 1982–83. Although these historically recent floods were robust, Rein (2007) suggests that they were not as large as El Niño floods that occurred during the Early or Late Holocene in coastal Peru. Similarly, despite the magnitude of the large ENSO-related floods that have occurred during the historical period, our stratigraphic and field evidence suggests that they have paled in comparison to the Late Quaternary floods presented herein. For example, the 1997–98 El Niño was perhaps the strongest El Niño of the 20th century (McPhaden, 1999); yet despite its elevated SOI (Southern Oscillation Index), the flooding in the Moquegua Valley corresponded to perhaps an estimated 50-year flood (Magilligan and Goldstein, 2001), and minimal sedimentological evidence of its occurrence was detected in any of the ephemeral channels to the mainstem Rio Moquegua. This is in strong contrast to the array of fluvial and debris flow deposits associated with stronger Niños that have occurred during the Late Pleistocene and Holocene. In a detailed reconstruction of El Niño frequency over the past 450 years, Quinn et al. (1987) showed that at least 17 "Strong" or "Very Strong" El Niños have occurred since ca. 1500, yet these extreme ENSOs have barely manifested geomorphologically in the Rio Moquegua watershed. For example, the modern channel along lower Rio Muerto is ~3 m wide in

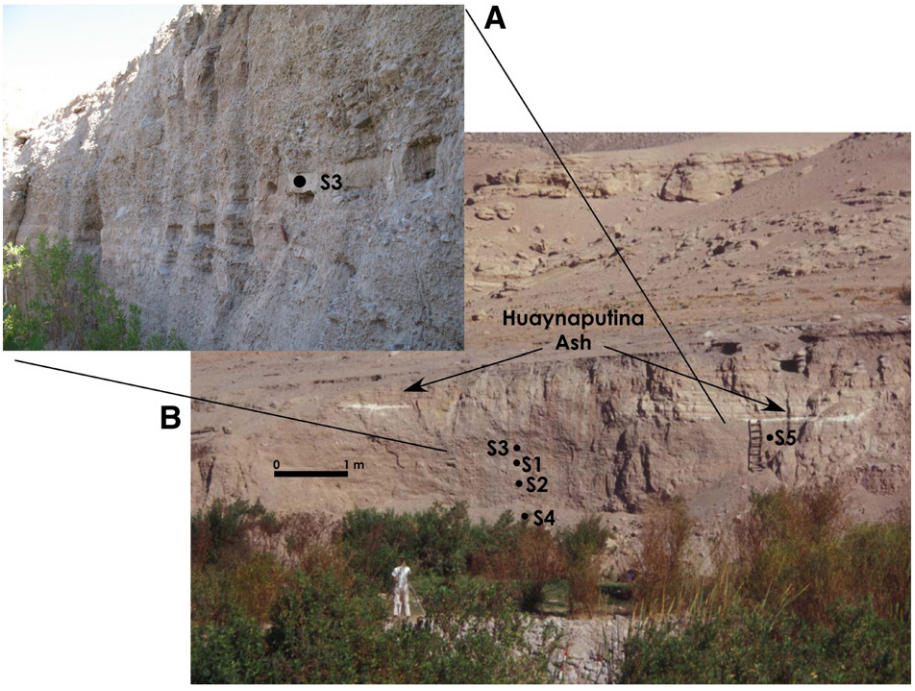

Fig. 11. Photos of the Slackwater site. Upper picture (A) is view from the left bank floodplain of the mainstem across the fan face showing the recent truncation of the fan face. Lower photo (B) shows fan stratigraphy and the slackwater rhythmites above the Huaynaputina ash of 1600 AD. S1–S5 refer to location of OSL samples (see Table 4 for OSL dates).

one dated section: the right bank has an upper flood unit dated to the Miraflores flood of ca. 1350 AD while the adjacent left bank has a basal date of 5590 cal yr AD. These observations suggest that the frequent El Niños documented by Quinn et al. (1987) have had little effect on tributary channels and that the kinds of events recorded stratigraphically indicate unusually large El Niños ranging in scale between the commonly occurring El Niños of every 8 years, on average, to the mega-Niños like the Miraflores flood. Our stratigraphic evidence suggests a strong variation in both flood intensity and occurrence during the past ca. 20,000 years and indicates several mega-Niños over the past 5600 years that spawned massive floods. For the Rio Muerto watershed, dated stratigraphic evidence suggests mega-Niños at ca. 5590 cal yr BP, 2120 cal yr BP, 1220 cal yr BP, and 400 cal yr BP with the Miraflores flood occurring somewhere between 700 and 600 cal yr BP.

5.4. Watershed scale hydrologic variation and climatic significance

Regional differences in the isotopic composition of moisture sources can potentially be used to provide information about the source and history of regional groundwater recharge and evolution. Aravena et al. (1999) have shown that considerable variation exists with altitude across the Andes: in general a depletion of ^{18}O occurs that results in more negative isotopic $\delta^{18}O$ values in the higher altitudes because of the extensive rainout of the Atlantic-sourced waters, while lower west side Andean water is enriched in ^{18}O in part because of rain evaporation, the degree of convection, and influence of nearby Pacific-sourced air masses. Our data show that distinct compositional differences exist between groundwater and surface water (Fig. 15A) and, similarly, that a strong elevational gradient exists for $\delta^{18}O$ for Andean west side surface waters (Fig. 15B). The depletion of $\delta^{18}O$ for waters from our locations is significantly less than that reported for highland Chilean precipitation and streamflow where Atlantic and Amazonian moisture sources control the isotopic composition (Aravena et al., 1999). Our surface water $\delta^{18}O$ values do, however, correspond to mid-elevation (~2000 m) precipitation derived primarily from Pacific moisture sources (Aravena et al., 1999). The $\delta^{18}O$ values cluster into two broad groups, (1) the mid- and upper-valley ground and surface waters, and (2) the downstream groundwater samples lower in the valley. This clustering implies that these two regions have

Table 4
Optically stimulated luminescence (OSL) dates

Sample	Lab ID #	U (ppm)	Th (ppm)	*K* (%)	Cosmic rate (Gy/ka)	Dose rate (Gy/ka)	Mean paleodose (Gy)	Mean age(ka)[a]	Height above river (m)
Slackwater S#5	UGA07OSL-523	2.45±0.54	8.29±1.87	2.24	0.1621	3.2±0.3	67.99±11.22	21.3±3.9	6
Slackwater S#3	UGA07OSL-508	1.87±0.33	6.61±1.16	1.99	0.1512	2.7±0.2	55.93±7.61	20.6±3.2	5.55
Slackwater S#1	UGA07OSL-440	2.20±0.49	7.15±1.67	2.08	0.1324	3.1±0.2	55.07±6.85[b]	18.9±2.8[b]	5.06
Slackwater S#2	UGA07OSL-439	2.16±0.47	6.85±1.62	2.12	0.1324	3.2±0.2	61.14±7.26	21.0±3.0	4.26
Slackwater S#4	UGA07OSL-509	1.94±0.48	7.42±1.63	1.95	0.1077	2.7±0.2	47.25±9.81	17.5±3.9	3.06
Tres Quebradas Fan	UGA07OSL-449	2.53±0.45	7.75±1.55	2.41	0.1264	3.6±0.2	53.59±12.75	16.2±4.1	8.15
Conde High Terrace (S#1)	UGA07OSL-441	3.23±0.42	5.5±1.49	2.25	0.1512	3.5±0.2	11.9±2.76	3.4±0.8	3.00

	Younger mode (6 aliquots)		Older mode (4 aliquots)	
	Mean paleodose (Gy)	Mean age (ka)	Mean paleodose (Gy)	Mean age (ka)
Slackwater S#1	55.07±6.84	18.9±2.8	95.08±7.88	32.7±3.8

[a] Assumes water content of 10%±5%.
[b] Slackwater S#1 has a bimodal distribution:

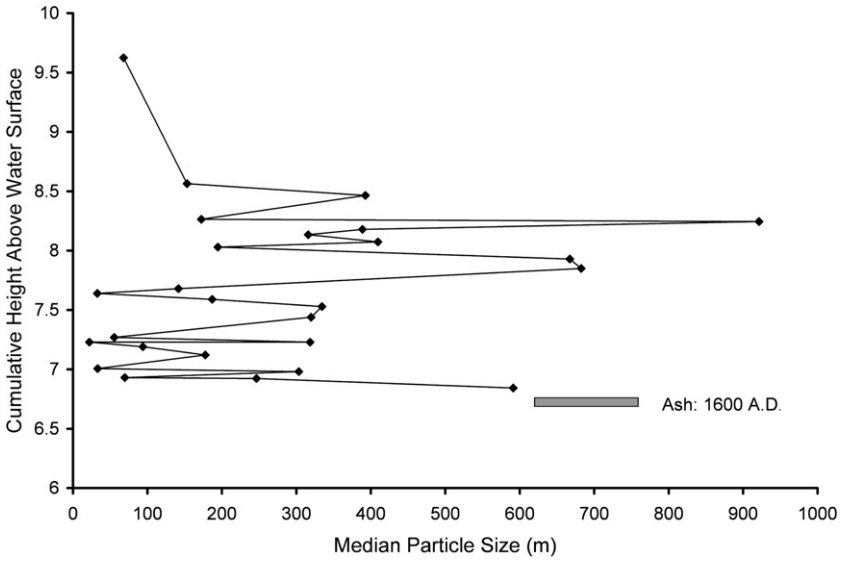

Fig. 12. Particle size of the slackwater sediments.

distinct aquifer systems and mechanisms of recharge. Trace element and DIC concentrations (Table 5) can further separate upper- and mid-valley surface waters from mid-valley groundwater. Of the 22 elements analyzed, significant differences emerged between downstream springs and either mid-valley wells or surface water samples for Fe, Na, S, and Sr. The elevated levels of these constituents indicate they have been impacted by more chemical weathering and thus suggest significantly older water. The similar oxygen isotopic composition between surface and groundwater from the upper- and mid-valley suggest a common source. In contrast, enriched $\delta^{18}O$ values in more distal groundwaters implies a very different moisture source that has been altered by weathering processes, evaporation, or locally enriched groundwater inflow. Overall, these data indicate that groundwaters in the entire region are sourced from Pacific moisture; thus, recharge is probably limited to major El Niño-related floods which bring extensive Pacific-sourced moisture to the region. Moreover, the distinct, individual isotopic composition for the spring near Cerro Baul (2400 masl) suggests that it is fossil groundwater not currently being recharged by contemporary precipitation; this lack of contemporary recharge is further supported by the significantly older age for this water with a ^{14}C age of 10,320 BP, while mid-valley wells and springs date to 710 BP and 3100 BP, respectively (Table 1; Fig. 15A). The relationship between δD and $\delta^{18}O$ also provides insight into the extent of evaporation within a specific water source. The surface waters of Rio Moquegua and its tributaries show a consistent relationship between δD and $\delta^{18}O$ ($\delta D = -27.4 + 5.8\ \delta^{18}O$, $R^2 = 0.69$). The shallow slope relative to the regional meteoric water line (MWL, slope = 7.8, Aravena et al., 1999) implies that these waters are considerably impacted by

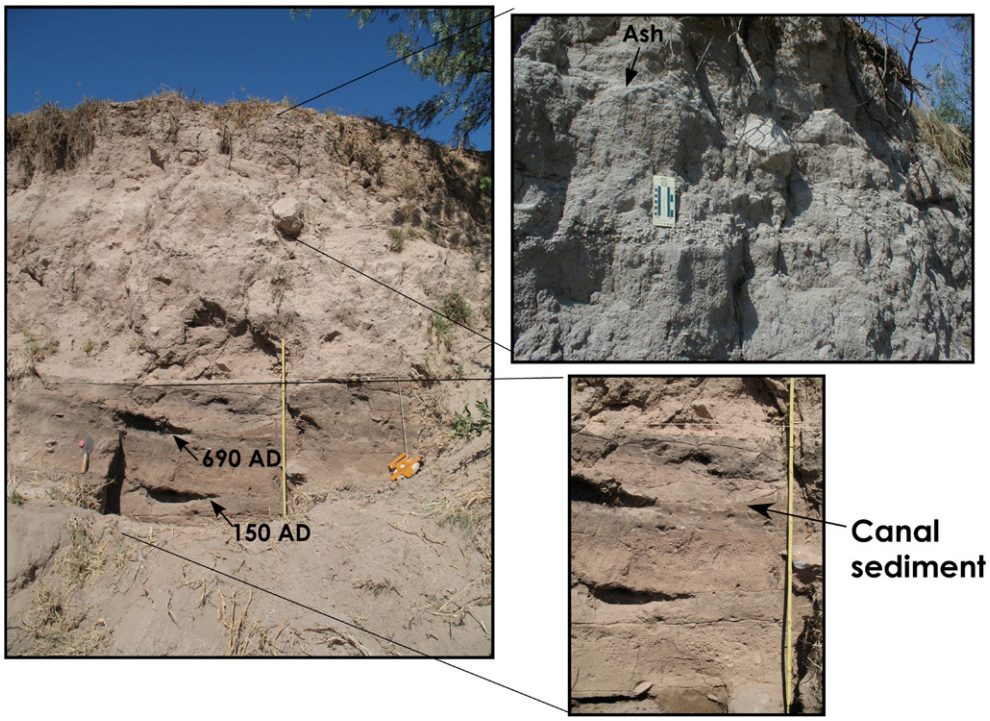

Fig. 13. Pictures of flood units within the Conde High Terrace.

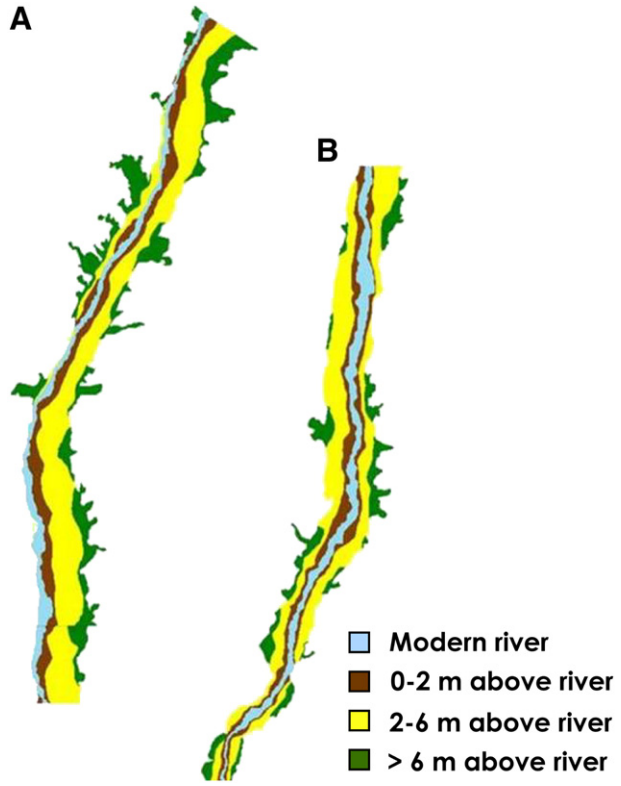

Fig. 14. Map of elevations of alluvial surfaces above active channel in the mid-valley of the Rio Moquegua. Figure on left (A) is the upper 9.9 km of the valley and (B) shows the lower 9.9 km.

evaporation along the flow path. In contrast, the $\delta^{18}O$ and δD values of lower elevation springs have $\delta^{18}O$ and δD (~−2‰ and −13‰ respectively) that vary from surface waters considerably but on a regression line of all isotopic data. These data suggest that they are derived from Pacific-derived moisture following little apparent evaporation, but also indicate that they represent a separate aquifer that is sourced from distinct recharge events.

In terms of other paleoclimatic indices other than flooding history, the geochemical data from the XRD analysis suggests both significant changes in climate and/or the impact of irrigation. The change in the percent calcite with depth at the Conde High Terrace (Fig. 16) indicates the relative changes in aridity or possibly the initiation of intensified irrigation. Prior to ca. 690 AD, background levels of calcite are all less than 1% with many samples lacking any calcite, especially between cal 150 and 690 AD (Fig. 16). In concert with this lack of calcite, the lack of sedimentation in this interval and the relatively high organic matter content of this material suggest a period of stability and lack of overbank flooding. Several reasons exist to explain this pattern: the low calcite content and lack of overbank flooding suggest wetter conditions to limit calcite production but at the same time not wet enough to generate large floods. Another possibility is that the low values of calcite and minimal sedimentation suggest a period of minimal flooding. After cal 690 AD, background levels of calcite increase dramatically toward the surface and unlike the period prior to 690 cal yr AD where calcite was always <1%, calcite in the period after cal AD 690 ranges between 1 and 4.3%. The elevated levels of calcite in the upper profile may reflect a post 700 AD climate change. However, our identification of early canal development at this same time at the Conde High Terrace suggests that the elevated calcite results more from irrigated agriculture on the floodplain. The maximum value corresponds to the surface unit which has been irrigated for several hundred years and has probably not been inundated since the Chuza flood of 1607 AD.

The correlation of the onset of increased levels of calcite with the Middle Horizon Tiwanaku colonization may not be coincidental. First, Tiwanaku settlement may correspond with a wetter period in the valley and increased use of spring sources recharged by Pacific-sourced rainfall. Secondly, the Tiwanaku state greatly expanded the agricultural base with the reclamation of extensive desert areas and increased reliance on springs, conditions that may correspond with anthropogenic salinization. While valley-bottom floodplain soils experienced fewer problems, present-day farmers experience significant problems of salts and calcite deposits when new desert areas are brought into cultivation, often requiring seasons of over-irrigation or mineral-resistant crops to "wash" new lands. Simultaneous upvalley development of new lands under terraced agricultural systems by the Wari polity could have exacerbated the problem, and brought on a permanent shift to higher levels of calcite.

5.5. Culture history, agrarian economics and climate change in the Moquegua Valley

In a region where multiple agrarian niches were used both over time and simultaneously by different cultural populations, associating the cultural effects of El Niños is extremely difficult and a subject of great debate (cf. Ortloff and Kolata, 1993; Erickson, 1999; Kolata et al., 2000; Erickson, 2000). Locally, El Niño floods, specifically the massive Miraflores event, are prime suspects in the collapse of the coastal valley Chiribaya culture in the 14th century (Moseley et al., 1983; Clement and Moseley, 1991; Moseley, 1997, 2000; Reycraft, 2000; Satterlee et al., 2000; Williams, 1997, 2002). The Miraflores event appears to have had a similarly catastrophic effect on Chiribaya agricultural systems and settlement at the Yaral choke point in mid-valley Moquegua, but farther upvalley may have had less impact on competing Late Intermediate polities; perhaps a competitive advantage that figured in their eventual takeover of the mid-valley following the Chiribaya.

While it is tempting to apply catastrophic scenarios to earlier floods, our understanding of regional settlement patterns and culture history suggest both negative and beneficial effects in complex multicultural interaction, rather than one universal effect. Our case in point is the transition from Late Formative simple valley-bottom agricultural systems to the massive colonization and agricultural expansion of the Tiwanaku in the Middle Horizon around spring-supplemented sources. Elsewhere, we have detailed that farmers in the valley bottom like the Huaracane of the Late Formative had to adapt to a mechanism of river channel migration and floodplain loss as a regular part of simple floodplain agriculture (Manners et al., 2007). Channel widening during floods erodes productive land and requires several decades to re-constitute to arable land, with a minimum of 30 years before the new alluvial material can be converted to productive land assuming of course that no intervening events occur (Manners et al., 2007). Conversely, populations entirely dependent on the valley-bottom planting surfaces may have found their adaptation untenable after repeated extreme ENSO events without intervening recovery time, or a single beyond-threshold "Mega-niño" flood, like that suggested by the 1220 BP (AD 730) event. Without their floodplain planting platform or a viable alternative strategy, Huaracane populations would have been forced to migrate or gone into debt peonage, serving more successful neighbors. With the young dates for mid-valley spring water, we can now posit that the same floods that were disastrous for the valley-bottom agrarian niche cleared the way for the Tiwanaku to exploit newly-recharged spring systems with large colonial settlements after ca. 700 AD.

Not only is Moquegua mid-valley precipitation significant in amount during El Niños, but these events tend to also have long durations lasting upwards of several months. These long duration events may have recharged local aquifers, and provided groundwater for adjacent springs that may offer opportunities for irrigated agriculture at elevations well above the valley-bottom floodplain. Radiocarbon dates on groundwater in the Moquegua Valley indicate

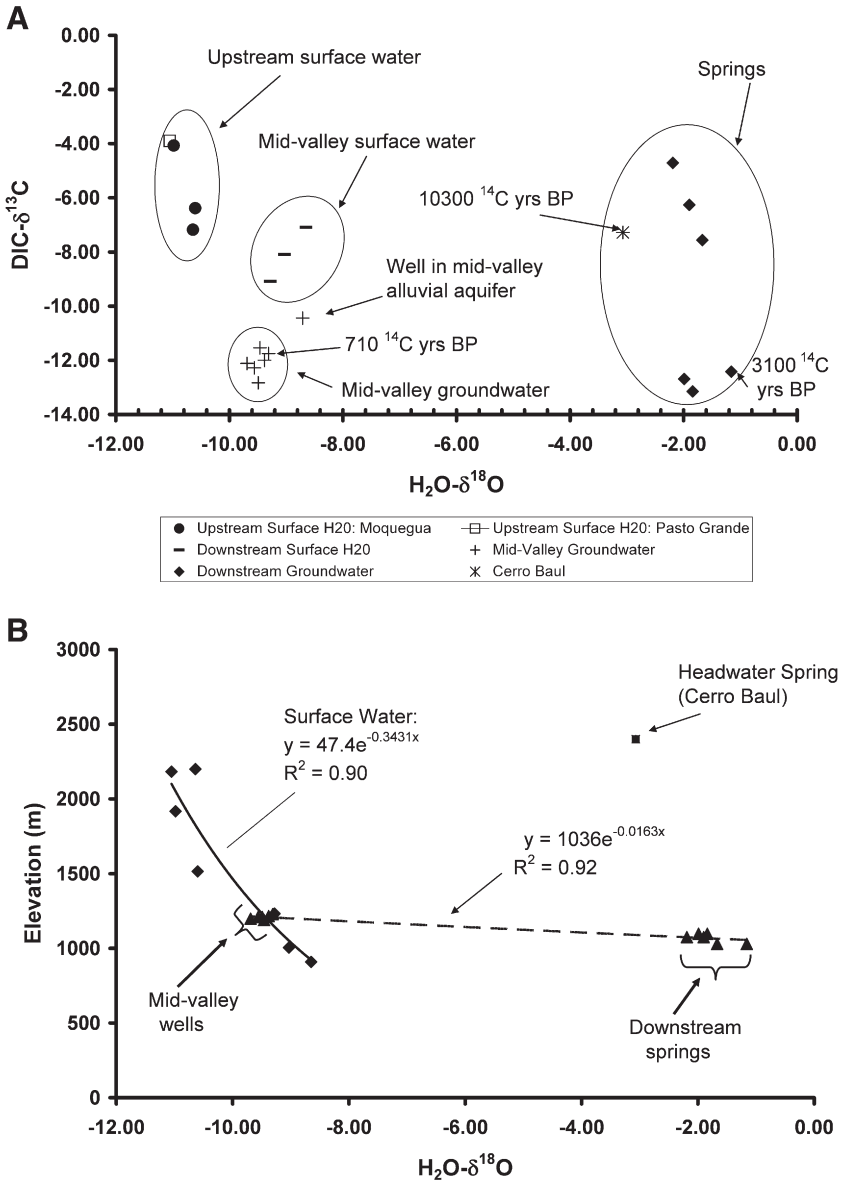

Fig. 15. Isotopic characteristics of surface water and groundwater. Upper diagram (A) plots the $\delta^{13}C$ of dissolved inorganic carbon (DIC) against $\delta^{18}O$. Bottom diagram is a plot of $\delta^{18}O$ composition of river water (solid line) and ground water (dashed line) but not including the headwater spring at Cerro Baul.

relatively young ages with water from the Zapata Well, adjacent to the enormous Tiwanaku settlement at Omo (Goldstein, 2005), dating to at least 710 ^{14}C years BP (Table 1). Although this date indicates that aquifers are not recharged on yearly or decadal scales, it suggests that the groundwater in this part of the valley is not fossil water from the Late Pleistocene. This contrasts sharply with a date of 10.3 ka (Table 1) for a groundwater sample from the flanks of Cerro Baul (S17° 07' 26.6″, W70° 50' 42.9″, 2000 masl), a major Wari occupation site. This older date near Cerro Baul suggests that some highland sources near the headwaters result from more fossil water from wetter conditions on the Altiplano and are not recharged from local precipitation. The date of 710 ^{14}C BP for the lower elevation mid-valley is somewhat older than recharge rates across the Chilean Altiplano where (Houston, 2007) has shown recharge rates to be on the order of ~40 years but it does indicate the important role of localized precipitation. In a more distant location in mid-elevations of the southern Atacama Desert, Squeo et al. (2006) have shown that water tables recover very quickly following El Niño events and indicate that local precipitation plays a significant role in groundwater recharge in these arid watersheds. The importance of El Niño episodes to groundwater recharge is poorly understood, but our data support a correlation of significant El Niño flooding with the sudden appearance of huge Tiwanaku agrarian colonies in the early 8th century AD, and the success of that colony's new agrarian niche dependent on spring-fed irrigation.

6. Conclusions

The variation in El Niño intensity and occurrence has been profound during the Late Quaternary as evidenced by the variation in the frequency and magnitude of large floods within the Rio Moquegua watershed. Although flooding is rare in these hyper-arid environments, the minimal re-working during normal years is absent, thus these watersheds provide a remarkable archive of paleofloods. In combination with the geochemical data of groundwater and streamflow, this paleoflood record indicates the broader hydrologic controls across the Atacama Desert of southern Peru.

In terms of Quaternary climate change, these tributary watersheds reveal intensified El Niño floods during the LGM and up to at least the Younger Dryas (ca. 12 ka cal yr BP) and then a significant absence of large El Niño floods until ca. 5590 cal yr BP suggesting that the Mid-Holocene was a protracted dry period across the Peruvian

Table 5
Results from water geochemistry for surface water, wells in the mid-valley of the Rio Moquegua, and springs at the lower end of the mid-valley (concentration in ppm)

	Ca	Cu	Fe	Li	Mg	Mn	Na	Ni	S	Sr
A. Surface waters										
Rio Huaracana	33.730	0.001	0.004	0.104	4.627	0.001	32.997	−0.003	20.138	0.276
Rio Tumilaca	19.264	0.001	0.009	0.014	3.333	0.001	12.729	−0.003	17.426	0.144
Rio Torato	33.604	0.003	0.010	0.020	4.561	−0.001	20.153	−0.005	12.297	0.265
Pasto Grande	17.801	−0.004	0.004	0.121	3.943	0.001	24.807	−0.003	17.223	0.150
Rio Moquegua - Montalvo	99.944	−0.003	0.009	0.078	11.777	0.007	88.072	−0.004	59.414	0.794
Rio Moquegua - near Conde	121.147	−0.013	0.007	0.071	18.505	−0.001	105.654	−0.002	72.968	0.921
Rio Moquegua - Yaral-1	121.126	−0.013	0.003	0.073	20.714	−0.001	129.398	−0.001	89.765	1.038
Average	63.802	−0.004	0.007	0.069	9.637	0.001	59.116	−0.003	41.319	0.513
Standard deviation	47.952	0.007	0.003	0.040	7.404	0.003	47.387	0.001	31.934	0.389
B. Headwater spring										
Cerro Baul	70.080	0.003	−0.005	0.006	0.110	−0.010	57.694	−0.088	57.724	0.538
C. Mid-valley wells										
Biondi #1	102.887	0.000	0.004	0.070	10.508	−0.002	98.752	−0.004	45.630	0.579
Biondi #2	107.929	−0.007	0.005	0.071	10.406	−0.001	98.962	−0.002	45.637	0.590
Biondi #3	112.154	−0.004	0.002	0.074	10.606	−0.002	111.337	−0.003	48.888	0.627
Biondi #4	110.377	−0.011	0.003	0.069	9.814	−0.003	96.503	−0.004	44.439	0.609
Zapata #2	129.404	−0.005	0.003	0.077	11.768	−0.002	96.567	−0.003	48.564	0.720
Zapata #3	127.571	−0.007	0.002	0.077	11.795	0.000	96.984	−0.003	48.571	0.713
Andrew's Well	307.019	−0.021	0.003	0.182	36.706	−0.001	227.500	−0.002	153.647	2.474
Average	142.477	−0.008	0.003	0.089	14.515	−0.002	118.086	−0.003	62.197	0.902
Standard deviation	73.232	0.007	0.001	0.041	9.813	0.001	48.530	0.001	40.365	0.696
D. Downstream springs										
Pterodactyl 1	175.960	0.011	0.000	0.478	4.174	−0.002	695.177	−0.002	264.967	2.777
Pterodactyl 2	237.201	0.006	0.000	0.547	6.037	−0.002	805.969	−0.003	343.739	3.729
Foxpath 1	608.271	0.012	0.030	0.561	38.947	0.245	604.179	0.006	734.256	6.289
Foxpath 2	602.955	−0.032	0.006	0.529	36.300	0.005	565.293	0.000	723.509	6.090
White Ruins #1	600.345	−0.029	0.092	1.887	51.168	0.001	2643.170	0.001	1472.378	7.925
White Ruins #2	586.781	−0.029	0.036	1.673	46.636	0.000	2513.743	0.000	1442.458	7.848
Average	468.585	−0.010	0.028	0.946	30.543	0.041	1304.588	0.000	830.218	5.776
Standard deviation	203.993	0.022	0.035	0.650	20.416	0.100	991.059	0.003	522.298	2.119
E. Results from t-test										
Surface Waters vs. wells	**0.04**	0.29	**0.03**	0.38	0.32	**0.04**	**0.04**	0.86	0.31	0.23
Surface waters vs. downstream springs	**0.00**	0.52	0.20	**0.02**	**0.05**	0.37	**0.03**	**0.05**	**0.01**	**0.00**
Wells vs. downstream springs	**0.01**	0.81	0.15	**0.02**	0.12	0.34	**0.03**	**0.05**	**0.02**	**0.00**

Bottom section of table (E) shows the significance level of *t*-test comparisons (**bold** indicates a significant (at $p=0.05$) relationship).

Atacama Desert. Moreover, the Late Holocene is a period of flooding intensification on the whole combined with catastrophic scale floods occurring ca. 1350 AD (the Miraflores flood) and ca. 1650 (the Chuza flood). For mainstem floods, these systems provide excellent records of ENSO activity although it is not possible to separate El Niño from La Niña episodes, unless dated stratigraphic units correspond such as ca. 2200 cal yr BP and both the Chuza and Miraflores floods. Evidence for an extreme La Niña flood comes from the most downstream site of the alluvial Rio Moquegua where a flood with an estimated discharge between 13,000 and 20,000 m^3/s occurred ca. 4200 cal yr BP. The lack of stratigraphic evidence of this flood in tributary sections suggests an origin in the Andean highlands and a probable La Niña event.

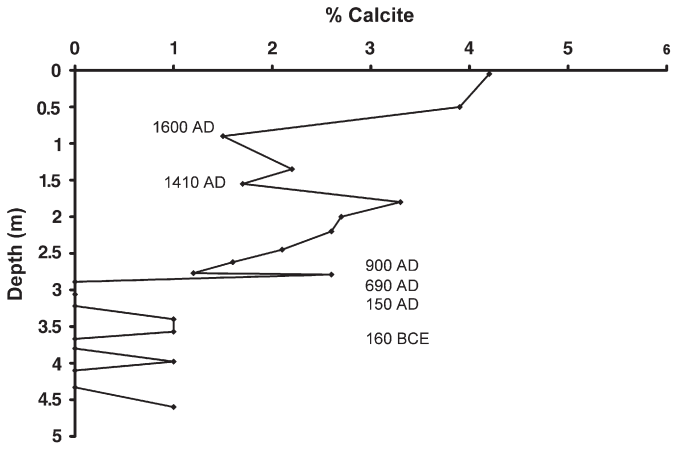

Fig. 16. Changes in percent calcite with depth at the Conde High Terrace.

Water chemistry and isotopic data further substantiate the important role of El Niño in the regional hydrology both on contemporary scales and during the Holocene. Besides the catastrophic nature of these ENSO episodes, their occurrence plays an important role in alluvial aquifer recharge. The depletion of $\delta^{18}O$ for waters from sites throughout a 1600 m elevational range in the Moquegua valley is significantly less than isotopic data reported for highland Chilean precipitation and streamflow where both Atlantic and Amazonian moisture sources control the isotopic composition (Aravena et al., 1999). Because our surface water $\delta^{18}O$ values correspond to mid-elevation (~2000 m) precipitation derived primarily from Pacific moisture sources (Aravena et al., 1999), we believe that the advection of Pacific moisture sources during El Niños is an important moisture source that has a fundamentally important role in recharging aquifers and thus may provide a sustained source of water well after the event. Thus El Niños have a catastrophic dimension associated with floodplain stripping (Manners et al., 2007), erosion of important irrigation canals (Huckleberry, 1999; Huckleberry and Billman, 2003), and wiping out villages (Keefer et al., 2003), but they also can provide cultural opportunities and serve a vital role in replenishing and maintaining groundwater resources across the Atacama Desert.

Acknowledgements

This research benefited from the kind support of the Dartmouth College Dickey Center for International Understanding (F. Magilligan,

R. Manners) and from the Dartmouth College Rockefeller Center (F. Magilligan). We would like to thank the editors, Paul Hudson, Tim Beach, and Karl Butzer for their guidance but especially their patience. The input from three anonymous reviewers greatly improved the quality and coherence of the paper. Additional thanks go to the University of California Pacific Rim Research Program and H.J. Heinz Foundation (P. Goldstein) and the Museo Contisuyo, Moquegua. Lastly, we greatly appreciate the efforts of Jodie Davi and Heather Carlos for figure preparation and the generous use of lab facilities provided by Peter Ryan and Patricia Manley at Middlebury College.

References

Abbott, M.B., Wolfe, B.B., Wolfe, A.P., Seltzer, G.O., Aravena, R., Mark, B.G., Polissar, P.J., Rodbell, D.T., Rowe, H.D., Vuille, M., 2003. Holocene paleohydrology and glacial history of the central Andes using multiproxy lake sediment studies. Palaeogeogr. Palaeoclimatol. Palaeoecol. 194 (1–3), 123–138.

Abbott, M.B., Binford, M.W., Brenner, M., Kelts, K.R., 1997a. A 3500 C-14 yr high-resolution record of water-level changes in Lake Titicaca, Bolivia/Peru. Quat. Res. 47 (2), 169–180.

Abbott, M.B., Seltzer, G.O., Kelts, K.R., Southon, J., 1997b. Holocene paleohydrology of the tropical Andes from lake records. Quat. Res. 47 (1), 70–80.

Alpers, C.N., Brimhall, G.H., 1988. Middle Miocene climatic change in the Atacama Desert, northern Chile: Evidence from supergene mineralization at La Escondida. Geol. Soc. Amer. Bull. 100, 1640–1656.

An, S.I., Timmermann, A., Bejarano, L., Jin, F.F., Justino, F., Liu, Z., Tudhope, A.W., 2004. Modeling evidence for enhanced El Niño-Southern Oscillation amplitude during the Last Glacial Maximum. Paleoceanography 19, PA4009. doi:10.1029/2004PA001020.

Aravena, R., Suzuki, O., Pefia, H., Pollastri, A., Fuenzalida, H., Grilli, A., 1999. Isotopic composition and origin of the precipitation in Northern Chile. Appl. Geochem. 14 (4), 411–422.

Baker, P.A., Seltzer, G.O., Fritz, S.C., Dunbar, R.B., Grove, M.J., Tapia, P.M., Cross, S.L., Rowe, H.D., Broda, J.P., 2001. The history of South American tropical precipitation for the past 25,000 years. Science 291 (5504), 640–643.

Betancourt, J.L., Latorre, C., Rech, J.A., Quade, J., Rylander, K.A., 2000. A 22,000-year record of monsoonal precipitation from Northern Chile's Atacama Desert. Science 289 (5484), 1542–1546.

Clarke, J.D.A., 2006. Antiquity of aridity in the Chilean Atacama Desert. Geomorphology 73 (1–2), 101–114.

Clement, C.O., Moseley, M.E., 1991. Spring-fed irrigation system of Carrizal, Peru: a case study of the hypothesis of agrarian collapse. J. Field Archaeol. 18, 425–443.

Cobb, K.M., Charles, C.D., Cheng, H., Edwards, R.L., 2003. El Niño/Southern Oscillation and tropical Pacific climate during the last millennium. Nature 424 (6946), 271–276.

Costa, J.E., 1983. Paleohydraulic reconstruction of flash-flood peaks from boulder deposits in the Colorado front range. Geol. Soc. Amer. Bull. 94 (8), 986–1004.

Cross, S.L., Baker, P.A., Seltzer, G.O., Fritz, S.C., Dunbar, R.B., 2000. A new estimate of the Holocene lowstand level of Lake Titicaca, central Andes, and implications for tropical palaeohydrology. Holocene 10 (1), 21–32.

deFrance, S.D., Keefer, D.K., 2005. Quebrada Tacahuay, southern Peru: a Late Pleistocene site preserved by a debris flow. J. Field Archaeol. 30 (4), 385–399.

DeVries, T.J., Ortlieb, L., Diaz, A., Wells, L., HillaireMarcel, C., 1997. Determining the early history of El Niño. Science 276 (5314), 965–966.

Diaz, H.F., Stahle, D.W., 2007. Climate and cultural history in the Americas: an overview. Clim. Change 83 (1–2), 1–8.

Dillehay, T.D., Kolata, A.L., 2004. Long-term human response to uncertain environmental conditions in the Andes. Proc. Natl. Acad. Sci. U. S. A. 101 (12), 4325–4330.

Donnelly, J.P., Woodruff, J.D., 2007. Intense hurricane activity over the past 5000 years controlled by El Niño and the West African monsoon. Nature 447 (7143), 465–468.

Drost, F., Renwick, J., Bhaskaran, B., Oliver, H., McGregor, J., 2007. Variability of the atmospheric circulation in the southern hemisphere during the Last Glacial Maximum. J. Geophys. Res.-Atmospheres 112 (D10), 11.

Dunai, T.J., Lopez, G.A.G., Juez-Larre, J., 2005. Oligocene-Miocene age of aridity in the Atacama Desert revealed by exposure dating of erosion-sensitive landforms. Geology 33 (4), 321–324.

Erickson, C.L., 1999. Neo-environmental determinism and agrarian 'collapse' in Andean prehistory. Antiquity 73 (281), 634–642.

Erickson, C.L., 2000. The Lake Titicaca Basin: a pre-Columbian built landscape. In: Lentz, D. (Ed.), Imperfect Balance: Landscape Transformations in the Precolumbian Americas. Columbia University, New York, pp. 311–356.

Ewing, S.A., Sutter, B., Owen, J., Nishiizumi, K., Sharp, W., Cliff, S.S., Perry, K., Dietrich, W.E., McKay, C.P., Amundson, R., 2006. A threshold in soil formation at Earth's arid–hyperarid transition. Geochim. Cosmochim. Acta 70 (21), 5293–5322.

Fisher, G.B., Ryan, P.C., 2006. The smectite-to-disordered kaolinite transition in a tropical soil chronosequence, Pacific coast, Costa Rica. Clays Clay Miner. 54 (5), 571–586.

Fontugne, M., Usselmann, P., Lavallee, D., Julien, M., Hatte, C., 1999. El Niño variability in the coastal desert of southern Peru during the Mid-Holocene. Quat. Res. 52 (2), 171–179.

Gagan, M.K., Hendy, E.J., Haberle, S.G., Hantoro, W.S., 2004. Post-glacial evolution of the Indo-Pacific Warm Pool and El Niño-Southern Oscillation. Quat. Int. 118–19, 127–143.

Garreaud, R.D., 1999. Multiscale analysis of the summertime precipitation over the central Andes. Mon. Weather Rev. 127 (5), 901–921.

Garreaud, R.D., 2000. Intraseasonal variability of moisture and rainfall over the South American Altiplano. Mon. weather rev. 128 (9), 3337–3346.

Garreaud, R.D., Aceituno, P., 2001. Interannual rainfall variability over the South American Altiplano. J. Climate 14 (12), 2779–2789.

Garreaud, R.D., Battisti, D.S., 1999. Interannual (ENSO) and interdecadal (ENSO-like) variability in the Southern Hemisphere tropospheric circulation. J. Climate 12 (7), 2113–2123.

Garreaud, R., Vuille, M., Clement, A.C., 2003. The climate of the Altiplano: observed current conditions and mechanisms of past changes. Palaeogeogr. Palaeoclimatol. Palaeoecol. 194 (1–3), 5–22.

Goldstein, P.S., 2000a. Exotic goods and everyday chiefs: long distance exchange and indigenous sociopolitical development in the south central Andes. Latin American Antiquity 11 (4), 1–27.

Goldstein, P., 2000b. Communities without borders — the vertical archipelago, and diaspora communities in the southern Andes. In: Yaeger, J., Canuto, M. (Eds.), The Archaeology of Communities: A New World Perspective. Routledge Press, pp. 182–209.

Goldstein, P., 2003. From stew-eaters to maize-drinkers: the Chicha Economy and Tiwanaku. In: Bray, T. (Ed.), Pots as Political Tools: The Culinary Equipment of Early Imperial States in Comparative Perspective. Kluwer Academic Publishers, New York, pp. 143–172.

Goldstein, P.S., 2005. Andean Diaspora: The Tiwanaku Colonies and the Origins of Andean Empire. University Press, Florida, Gainesville.

Gomez, B., Carter, L., Trustrum, N.A., Palmer, A.S., Roberts, A.P., 2004. El Niño Southern Oscillation signal associated with middle Holocene climate change in intercorrelated terrestrial and marine sediment cores, North Island, New Zealand. Geology 32 (8), 653–656.

Gregory-Wodzicki, K.M., 2000. Uplift history of the Central and Northern Andes: a review. Geol. Soc. Amer. Bull. 112 (7), 1091–1105.

Grosjean, M., van Leeuwen, J.F.N., van der Knaap, W.O., Geyh, M.A., Ammann, B., Tanner, W., Messerli, B., Nunez, L.A., Valero-Garces, B.L., Veit, H., 2001. A 22,000 C-14 year BP sediment and pollen record of climate change from Laguna Miscanti (23 degrees S), northern Chile. Glob. Planet. Change 28 (1–4), 35–51.

Grosjean, M., Cartajena, I., Geyh, M.A., Nunez, L., 2003. From proxy data to paleoclimate interpretation: the Mid-Holocene paradox of the Atacama Desert, northern Chile. Palaeogeogr. Palaeoclimatol. Palaeoecol. 194 (1–3), 247–258.

Hartley, A.J., Chong, G., 2002. Late Pliocene age for the Atacama Desert: implications for the desertification of western South America. Geology 30 (1), 43–46.

Hartley, A.J., Chong, G., Houston, J., Mather, A.E., 2005. 150 million years of climatic stability: evidence from the Atacama Desert, northern Chile. J. Geol. Soc. 162, 421–424.

Hastorf, C.A., Whitehead, W.T., Bruno, M.C., Wright, M.F., 2006. Movements of maize into middle horizon Tiwanaku, Bolivia. In: Staller, J.E., Tykot, R.H., Benz, B.F. (Eds.), Histories of Maize: Multidisciplinary Approaches to the Prehistory, Linguistics, Biogeography, Domestication, and Evolution of Maize. Elsevier Academic Press, Amsterdam, pp. 429–447.

Hillier, S., 1999. Use of an air brush to spray dry samples for X-ray powder diffraction. Clay Miner. 34 (1), 127–135.

Holmgren, C.A., Betancourt, J.L., Rylander, K.A., Roque, J., Tovar, O., Zeballos, H., Linares, E., Quade, J., 2001. Holocene vegetation history from fossil rodent middens near Arequipa, Peru. Quat. Res. 56 (2), 242–251.

Houston, J., 2007. Recharge to groundwater in the Turi Basin, northern Chile: an evaluation based on tritium and chloride mass balance techniques. J. Hydrol. 334 (3–4), 534–544.

Houston, J., Hartley, A.J., 2003. The central Andean west-slope rainshadow and its potential contribution to the origin of hyper-aridity in the Atacama desert. Int. J. Climatol. 23 (12), 1453–1464.

Huckleberry, G.A., 1999. Stratigraphic identification of destructive floods in relict canals: a case study from the middle Gila River, Arizona. Kiva 86, 7–33.

Huckleberry, G., Billman, B.R., 2003. Geoarchaeological insights gained from surficial geologic mapping, middle Moche Valley, Peru. Geoarchaeology—An International Journal 18 (5), 505–521.

Keefer, D.K., deFrance, S.D., Moseley, M.E., Richardson, J.B., Satterlee, D.R., Day-Lewis, A., 1998. Early maritime economy and EL Niño events at Quebrada Tacahuay, Peru. Science 281 (5384), 1833–1835.

Keefer, D.K., Moseley, M.E., deFrance, S.D., 2003. A 38 000-year record of floods and debris flows in the Ilo region of southern Peru and its relation to El Niño events and great earthquakes. Palaeogeogr. Palaeoclimatol. Palaeoecol. 194 (1–3), 41–77.

Knox, J.C., 2000. Sensitivity of modern and Holocene floods to climate change. Quat. Sci. Rev. 19 (1–5), 439–457.

Kolata, A.L., Binford, M.W., Brenner, M., Janusek, J.W., Ortloff, C., 2000. Environmental thresholds and the empirical reality of state collapse: a response to Erickson (1999). Antiquity 74 (284), 424–426.

Kumar, R., Nunn, P.D., Field, J.S., de Biran, A., 2006. Human responses to climate change around AD 1300: a case study of the Sigatoka Valley, Viti Levu Island, Fiji. Quat. Int. 151, 133–143.

Latorre, C., Betancourt, J.L., Arroyo, M.T.K., 2006. Late Quaternary vegetation and climate history of a perennial river canyon in the Rio Salado basin (22 degrees S) of Northern Chile. Quat. Res. 65 (3), 450–466.

Leigh, D.S., Srivastava, P., Brook, G.A., 2004. Late Pleistocene braided rivers of the Atlantic Coastal Plain, USA. Quat. Sci. Rev. 23 (1–2), 65–84.

Lenters, J.D., Cook, K.H., 1997. On the origin of the Bolivian high and related circulation features of the South American climate. J. Atmos. Sci. 54 (5), 656–677.

Lenters, J.D., Cook, K.H., 1999. Summertime precipitation variability over South America: role of the large-scale circulation. Mon. Weather Rev. 127 (3), 409–431.

Maas, G.S., Macklin, M.G., Warburton, J., Woodward, J.C., Meldrum, E., 2001. A 300 year history of flooding in an Andean mountain river system: the river Alizos, Southern

Bolivia. In: Maddy, D.A., Macklin, M.G., Woodward, J.C. (Eds.), River Basin Sediment Systems, pp. 297–323.
Magilligan, F.J., Goldstein, P.S., 2001. El Niño floods and culture change: a Late Holocene flood history for the Rio Moquegua, southern Peru. Geology 29 (5), 431–434.
Magilligan, F.J., Salant, N.L., Renshaw, C.E., Nislow, K.H., Heimsath, A., Kaste, J., 2006. Evaluating the impacts of impoundment on sediment transport using short-lived fallout radionuclides. In: Rowan, J., Werrity, A. (Eds.), Sediment Dynamics and The Hydromorphology of Fluvial Systems. The International Association of Hydrological Sciences (IAHS) Special Publication, vol. 306. IAHS Press, Wallingford, UK, pp. 159–165.
Manners, R., Magilligan, F.J., Goldstein, P.S., 2007. Floodplain development, El Niño, and cultural consequences in a hyperarid Andean environment. Ann. Assoc. Am. Geogr. 97 (2), 229–249.
Marchant, R., Hooghiemstra, H., 2004. Rapid environmental change in African and South American tropics around 4000 years before present: a review. Earth-Sci. Rev. 66 (3–4), 217–260.
Marocco, R., Noblet, C., 1990. Sedimentation, tectonism and volcanism relationships in 2 Andean basins of southern Peru. Geol. Rundsch. 79 (1), 111–120.
McPhaden, M.J., 1999. Genesis and evolution of the 1997–98 El Niño. Science 283 (5404), 950–954.
Meggers, B.J., 1994. Archaeological evidence for the impact of mega-Niño events on Amazonia during the past 2 millennia. Clim. Change 28 (4), 321–338.
Moseley, M.E., 1997. Climate, culture and punctuated change: new data, new challenges. Rev. Archaeol. 18, 19–27.
Moseley, M.E., 2000. Confronting natural disaster. In: Bawden, G., Reycraft, R.M. (Eds.), Environmental Disaster and the Archaeology of Human Response. Maxwell Museum of Anthropology, University of New Mexico, Albuquerque, pp. 219–223.
Moseley, M.E., Feldman, R.A., Ortloff, C.R., Narvaez, A., 1983. Principles of agrarian collapse in the Cordillera Negra, Peru. Ann. Carnegie Mus. 52, 299–327.
Nunn, P.D., 2000. Environmental catastrophe in the Pacific Islands around A.D. 1300. Geoarchaeology 15 (7), 715–740.
Ortloff, C.R., Kolata, A.L., 1993. Climate and collapse — agroecological perspectives on the decline of the Tiwanaku state. J. Archaeol. Sci. 20 (2), 195–221.
Peltier, W.R., Solheim, L.P., 2004. The climate of the Earth at Last Glacial Maximum: statistical equilibrium state and a mode of internal variability. Quat. Sci. Rev. 23 (3–4), 335–357.
Placzek, C., Quade, J., Betancourt, J.L., 2001. Holocene lake-level fluctuations of Lake Aricota, southern Peru. Quat. Res. 56 (2), 181–190.
Placzek, C., Quade, J., Patchett, P.J., 2006. Geochronology and stratigraphy of Late Pleistocene lake cycles on the southern Bolivian Altiplano: implications for causes of tropical climate change. Geol. Soc. Amer. bull. 118 (5–6), 515–532.
Quinn, W.H., Neal, V.T., Demayolo, S.E.A., 1987. El-Niño occurrences over the past 4-1/2 centuries. J. Geophys. Res.-Oceans 92 (C13), 14449–14461.
Rech, J.A., Pigati, J.S., Quade, J., Betancourt, J.L., 2003. Re-evaluation of Mid-Holocene deposits at Quebrada Puripica, northern Chile. Palaeogeogr. Palaeoclimatol. Palaeoecol. 194 (1–3), 207–222.
Rech, J.A., Currie, B.S., Michalski, G., Cowan, A.M., 2006. Neogene climate change and uplift in the Atacama Desert, Chile. Geology 34 (9), 761–764.
Rein, B., 2007. How do the 1982/83 and 1997/98 El Niños rank in a geological record from Peru? Quat. Int. 161, 56–66.
Rein, B., Luckge, A., Sirocko, F., 2004. A major Holocene ENSO anomaly during the Medieval period. Geophys. Res. Lett. 31 (17).
Rein, B., Luckge, A., Reinhardt, L., Sirocko, F., Wolf, A., Dullo, W.C., 2005. El Niño variability off Peru during the last 20,000 years. Paleoceanography 20 (4), 18.
Reycraft, R.M., 2000. Long-term human response to El Niño in South Coastal Peru, circa A.D.1400. In: Bawden, G., Reycraft, R.M. (Eds.), Environmental disaster and the Archaeology of Human Response. Maxwell Museum of Anthropology, University of New Mexico, Albuquerque, pp. 99–119.
Rice, D., 1993. Late Intermediate period domestic architecture and residential organization at La Yaral. In: Aldenderfer, M. (Ed.), Domestic Architecture, Ethnicity, and Complementarity in the South-Central Andes. University of Iowa Press, Iowa City, pp. 66–82.
Riedinger, M.A., Steinitz-Kannan, M., Last, W.M., Brenner, M., 2002. A similar to 6100 C-14 yr record of El Niño activity from the Galapagos Islands. J. Paleolimnol. 27 (1), 1–7.
Rodbell, D.T., Seltzer, G.O., Anderson, D.M., Abbott, M.B., Enfield, D.B., Newman, J.H., 1999. An similar to 15,000-year record of El Niño-driven alluviation in south-western Ecuador. Science 283 (5401), 516–520.
Rowe, H.D., Dunbar, R.B., Mucciarone, D.A., Seltzer, G.O., Baker, P.A., Fritz, S., 2002. Insolation, moisture balance and climate change on the South American Altiplano since the Last Glacial Maximum. Clim. Change 52 (1–2), 175–199.
Russell, J.M., Johnson, T.C., 2007. Little Ice Age drought in equatorial Africa: Intertropical Convergence Zone migrations and El Niño-Southern Oscillation variability. Geology 35 (1), 21–24.
Salant, N.L., Renshaw, C.E., Magilligan, F.J., Kaste, J.M., Nislow, K.H., Heimsath, A.M., 2007. The use of short-lived radionuclides to quantify transitional bed material transport in a regulated river. Earth Surf. Processes Landf. 32 (4), 509–524.
Sandweiss, D.H., Richardson, J.B., Reitz, E.J., Rollins, H.B., Maasch, K.A., 1996. Geoarchaeological evidence from Peru for a 5000 years BP onset of El Niño. Science 273 (5281), 1531–1533.
Sandweiss, D.H., Maasch, K.A., Burger, R.L., Richardson, J.B., Rollins, H.B., Clement, A., 2001. Variation in Holocene El Niño frequencies: climate records and cultural consequences in ancient Peru. Geology 29 (7), 603–606.
Satterlee, D.R., Moseley, M.E., Keefer, D.K., Tapia, J.E., 2000. The Miraflores El Niño disaster: convergent catastrophes and prehistoric agrarian change in southern Peru. Andean Past 6, 95–116.
Schimmelmann, A., Zhao, M., Harvey, C.C., Lange, C.B., 1998. A large California flood and correlative global climatic events 400 years ago. Quat. Res. 49 (1), 51–61.
Schimmelmann, A., Lange, C.B., Meggers, B.J., 2003. Palaeoclimatic and archaeological evidence for a similar to 200-yr recurrence of floods and droughts linking California, Mesoamerica and South America over the past 2000 years. Holocene 13 (5), 763–778.
Seltzer, G.O., Baker, P., Cross, S., Dunbar, R., Fritz, S., 1998. High-resolution seismic reflection profiles from Lake Titicaca, Peru-Bolivia: evidence for Holocene aridity in the tropical Andes. Geology 26 (2), 167–170.
Squeo, F.A., Aravena, R., Aguirre, E., Pollastri, A., Jorquera, C.B., Ehleringer, J.R., 2006. Groundwater dynamics in a coastal aquifer in north-central Chile: implications for groundwater recharge in an arid ecosystem. J. Arid Environ. 67 (2), 240–254.
Srodon, J., Drits, V.A., McCarty, D.K., Hsieh, J.C.C., Eberl, D.D., 2001. Quantitative X-ray diffraction analysis of clay-bearing rocks from random preparations. Clays Clay Miner. 49 (6), 514–528.
Stuiver, M., Reimer, P.J., 1993. Extended ^{14}C database and revised CALIB radiocarbon calibration program. Radiocarbon 35, 215–230.
Thompson, L.G., Mosleythompson, E., Bolzan, J.F., Koci, B.R., 1985. A 1500-year record of tropical precipitation in ice cores from the Quelccaya ice cap, Peru. Science 229 (4717), 971–973.
Thouret, J.C., Davila, J., Eissen, J.P., 1999. Largest explosive eruption in historical times in the Andes at Huaynaputina volcano, AD 1600, southern Peru. Geology 27 (5), 435–438.
Thouret, J.C., Juvigne, E., Gourgaud, A., Boivin, P., Davila, J., 2002. Reconstruction of the AD 1600 Huaynaputina eruption based on the correlation of geologic evidence with early Spanish chronicles. J. Volcanol. Geotherm. Res. 115 (3–4), 529–570.
Tosdal, R.M., Clark, A.H., Farrar, E., 1984. Cenozoic polyphase landscape and tectonic evolution of the cordillera occidental, southernmost Peru. Geol. Soc. Amer. Bull. 95 (11), 1318–1332.
Trenberth, K.E., 1997. The definition of El Niño. Bull. Am. Meteorol. Soc. 78 (12), 2771–2777.
Vuille, M., 1999. Atmospheric circulation over the Bolivian Altiplano during dry and wet periods and extreme phases of the Southern Oscillation. Int. J. Climatol. 19 (14), 1579–1600.
Vuille, M., Bradley, R.S., Keimig, F., 2000a. Climate variability in the Andes of Ecuador and its relation to tropical Pacific and Atlantic sea surface temperature anomalies. J. Climate 13 (14), 2520–2535.
Vuille, M., Bradley, R.S., Keimig, F., 2000b. Interannual climate variability in the Central Andes and its relation to tropical Pacific and Atlantic forcing. J. Geophys. Res.-Atmospheres 105 (D10), 12447–12460.
Wells, L.E., 1987. An alluvial record of El-Niño events from northern coastal Peru. J. Geophys. Res.-Oceans 92 (C13), 14463–14470.
Wells, L.E., 1990. Holocene history of the El-Niño phenomenon as recorded in flood sediments of northern coastal Peru. Geology 18 (11), 1134–1137.
Wells, L.E., Noller, J.S., 1997. Determining the early history of El Niño. Science 276 (5314), 966-966.
Williams, R.P., 1997. Disaster in the Development of Agriculture and the Evolution of Social Complexity in the South-Central Andes. Ph.D. Dissertation University of Florida.
Williams, R.P., 2002. Rethinking disaster-induced collapse in the demise of the Andean highland states: Wari and Tiwanaku. World Archaeol. 33, 361–374.